Tracking Holocene glacial and high-altitude alpine environments fluctuations from minerogenic and organic markers in proglacial lake sediments (Lake Blanc Huez, Western French Alps)

CrossMark

Anaëlle Simonneau [a,b,*], Emmanuel Chapron [a], Marion Garçon [c], Thierry Winiarski [d], Yann Graz [a,e], Catherine Chauvel [c], Maxime Debret [a,f], Mickaël Motelica-Heino [a], Marc Desmet [g], Christian Di Giovanni [a]

[a] Institut des Sciences de la Terre d'Orléans, UMR 7327, CNRS, Univ. Orléans, BRGM, 1A rue de la Férollerie, 45071 Orléans Cedex 2, France
[b] GEODE, UMR 5602 CNRS/Université de Toulouse 2, Allée A. Machado, 31058 Toulouse Cedex, France
[c] ISTerre, Université Joseph Fourier de Grenoble, BP 53, 38041 Grenoble cedex 09, France
[d] LEHNA-IPE UMR 5023, Ecole Nationale des Travaux Public de l'Etat, Université de Lyon, rue Maurice Audin, 69518 Vaulx-en-Velin, France
[e] Université de Lorraine, Institut Jean Lamour, UMR 7198, Vandoeuvre-lès-Nancy F-54506, France
[f] Laboratoire de Morphodynamique Continentale et Côtière, UMR 6143, Université de Rouen, France
[g] GéoHydrosystèmes Continentaux AE CNRS, Université François-Rabelais de Tours, Parc de Grandmont, 37200 Tours, France

ARTICLE INFO

ABSTRACT

Holocene palaeoenvironmental evolution and glacial fluctuations at high-altitude in the western French Alps are reconstructed based on a multiproxy approach within Lake Blanc Huez (2550 m a.s.l.) drainage basin. The combination of seismic profiling (3.5 kHz), piston coring and radiocarbon dating in proglacial lacustrine sediments together with a detailed organic analysis of autochthonous and allochthonous supply allows documenting the evolution of glacier activity during the Holocene. Over the last 9700 years, the Holocene lake record has a bimodal pattern whose transition is progressive and occurring between 5400 and 4700 cal BP. During the Early Holocene, the organic lacustrine facies reflects reduced glacial activity in the catchment. This major glacial retreat seems to result from solar forcing and high summer insolation. After 5400 cal BP, lacustrine sedimentation is marked by the gradual increase both of minerogenic supply and soil erosion, suggesting a progressive transition to wetter climatic conditions. This climate change is synchronous both from the gradual decrease of summer insolation and the gradual reorganization of oceanic and atmospheric circulations, characterizing the beginning of the Neoglacial period. Both colder temperature and humid climate induced significant glacier advance, since 4700 cal BP. Over this global trend, three periods are particularly associated with higher runoff processes and higher soil erosion interpreted as wetter time intervals resulting from enhanced northern Westerlies regimes across the North Atlantic and Western Europe. They are dated from 8700 to 7000, 4700 to 2500 and 1200 to 200 cal BP. These wetter phases drastically contrast with periods of reduced glacial activities dated from the Early Bronze Age (ca 3870−3770 cal BP), the Iron Age (ca 2220−2150 cal BP), the Roman period (ca AD115−330) and the Medieval Warm Period (ca AD760−1160). In addition, these dryer periods are associated with mining activities at high-altitude.

© 2014 Elsevier Ltd. All rights reserved.

1. Introduction

In order to better understand the potential effects of on-going climate change on continental environments, it is essential to disentangle the respective contributions of Holocene climate variability and the evolution of human activities on past environmental changes (Dearing and Jones, 2003; Magny, 2004; Desmet et al., 2005; Jungclaus et al., 2010). Glaciers are important climate indicators because their fluctuations are both sensitive to summer air temperature, winter precipitations and solar irradiance (Holzhauser et al., 2005; Vincent et al., 2005; Joerin et al., 2006). Over the past decades, Matthews and Karlén (1992), Leeman and Niessen (1994), Leonard (1997), Ariztegui et al. (1997) and Nesje

et al. (2001) have demonstrated in various mountain ranges that proglacial lakes can provide continuous high-resolution sedimentary records of past glacial fluctuations in their catchments. Bedrock abrasion by a temperate glacier is maximal at the equilibrium line altitude (ELA) of the glacier (Dahl et al., 2003) and produces fine rock and mineral fragments ("glacigenic" or "minerogenic" material). During summer months, a relatively large amount of silt- and clay-size particles originating from glacial abrasion is transported in suspension by glacial melt waters and is deposited into proglacial lakes. Because erosion rate increases with glacier size and thickness, variations over time in the accumulated amount of glacigenic (or minerogenic) material in proglacial lake sediments provides a reliable high-resolution record of glacier activity and thus, of climate changes. Conversely, gyttja deposits in proglacial lacustrine environments are rich in organic matter (OM) but poor in minerogenic material and reflect periods without any significant glacier activity in the drainage basin (Nesje et al., 2001). Because OM in lakes can have different origins (either algal production, soil erosion or bedrock erosion) and since OM accumulation and preservation can reflect climatic regimes and global climatic conditions (Lallier-Vergès et al., 1993; Ariztegui et al., 1996; Sifeddine et al., 1996; Simonneau et al., 2013a). It is relevant to clearly quantify and qualify the different sources of OM accumulated in a proglacial lacustrine sequence.

Nowadays, high-altitude alpine environments (>2000 m) are essentially affected by the development of ski industry, the production of hydroelectricity and global warming (Anselmetti et al., 2007; Chapron et al., 2007; Guyard et al., 2007). Recent studies also revealed that the expansion of copper exploitation by the action of fire started during the Bronze Age period (beginning around 4350 cal BP in the southern French Alps and around 4200 cal BP in the Western French Alps). Such mining activities were concentrated in small areas and may have been exploited several times in ancient times (Bailly-Maître and Bruno-Dupraz, 1994; Guyard et al., 2007; Bailly-Maître and Gonon, 2006; Carozza et al., 2009; Garçon et al., 2012). Thus, in addition to former pastoral activities at lower elevation sites (Chardon, 1991), the past development of metallurgy above 2000 m altitude may have affected the altitude of the treeline, paedological processes and/or runoff in this part of the Alps.

In the present paper, we document for the first time the evolution of glacier activity and soil erosion over the Holocene in a high-altitude (2500 m a.s.l.) proglacial lake from the western Alps (Fig. 1A) located on the windward side of the northern westerly wind belt originating from the Atlantic Ocean. Based on a
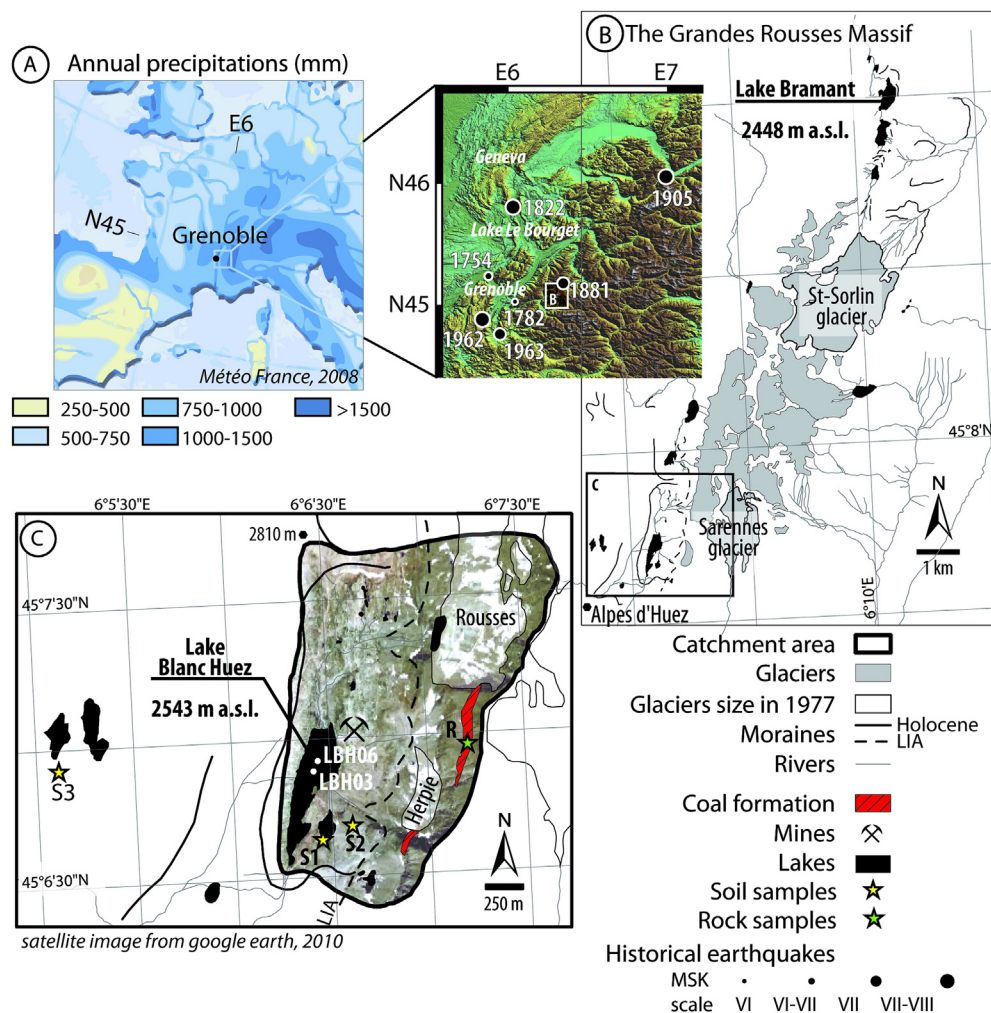

Fig. 1. Annual precipitation from Western Europe (A) and location of the Grandes Rousses massif in the active seismic zone of the western French Alps (B). Lake Blanc Huez is at the southern side of the Grandes Rousses massif (C). Its catchment area (thick black line, C) is partly covered by the Rousses and the Herpie glaciers. Their Little Ice Age (LIA, dashed line) and older Holocene moraines (thin black full line) are represented. As discussed in the text, the lake is also affected by human mining activities. The location of LBH06 piston core, three soil (S1, S2, S3, yellow stars) profiles and one rock sample from the Stephanian coal formation (R, green star) are also indicated in (C). (For interpretation of the references to colour in this figure legend, the reader is referred to the web version of this article.)

multiproxy study comparing lake sediments geometry, minerogenic parameters and geochemistry with specific organic markers on lake, soils and geological samples from the same catchment area, we first establish a stratigraphy for the proglacial lacustrine infill of Lake Blanc Huez (LBH). Because radiocarbon dating can be limited at high-elevation sites (i.e. located above the altitude of the tree-line), we then establish an age-depth model using AMS ^{14}C dating on vegetal remains and bulk sediments together with independent chronological markers such as local archaeological data and regional earthquakes. Finally, this approach produces a continuous sedimentary record of environmental changes at high-altitude since ca 10 000 years which opens the discussion on the respective contribution of climate and human activities on soil erosion in the Western French Alps.

2. Setting

2.1. Geography and geology

Lake Blanc Huez (LBH) is a small and narrow proglacial lake (880 m long, 350 m wide and 40 m deep) located at 2543 m above sea level (m a.s.l.) on the south western side of the Grandes Rousses massif in the Western French Alps (45°7′N—6°6′E, Fig. 1B). The catchment area of this lake (Fig. 1C) is small (3.2 km^2) and its bedrock consists in sedimentary and metamorphic rocks (gneiss, micaschist overlain by limestone and conglomerate) which are covered by glacial formations. These rocks are crossed cut by a stripe of Stefanian coal formation and are affected by faults which are filled with iron oxides (Barfety et al., 1972a,b). Lead-silver veins with quartz-barite gangue occur also in various places in the catchment. Alpine soils are recent, almost devoid of vegetation and underdeveloped because of steep snow-covered slopes more than six months per year (Flusin et al., 1909).

2.2. Glaciers and climatology

As shown in Fig. 1A, the Grandes Rousses massif is the first high-altitude mountain-range on the windward side of the northern westerly wind belt originating from the Atlantic Ocean and is subjected to rather high-precipitation regimes (>1500 mm pear year, Blanchet, 1994). This massif is characterized by numerous plateau and cirque glaciers present between 2500 and 3400 m a.s.l.. Two glaciers located on the southern (Sarennes) and northern (St Sorlin) side of the Granges Rousses massif (Fig. 1B) have been instrumented since AD1949 and AD1957, respectively, and are considered as representative for the NW Alpine region (Torinesi et al., 2002; Vincent, 2002). In AD2001, the glacier ELA (i.e. Equilibrium Line Altitude) was around 2900 m a.s.l. in the northern part of the massif. Since the 20th century, variations in temperate glacier ELAs are essentially controlled by mean summer temperatures (Vincent, 2002) but during the Little Ice Age (LIA, 15th—19th centuries) ELAs were driven by winter precipitation regimes (Vincent et al., 2005). In addition, decadal mass balance variations of French western alpine glaciers and Norwegian western glaciers have been out of phase since AD1960 and show good correlations with the North Atlantic Oscillation (NAO) index (Six et al., 2007), suggesting that the alpine climate, and in particular snow accumulations, are closely influenced by the westerly winds and the Atlantic ocean (Wanner et al., 2008; Marzeion and Nesje, 2012; Guyard et al., 2013).

2.3. Moraines

Five generations of former moraine belts were mapped in the Grandes Rousses massif by Flusin et al. (1909) and Montjuvent and

Chardon (1989) between 1700 and 2600 m a.s.l. (Fig. 1B). The two oldest ones were recognized below LBH, near the ski resort of Alpe d'Huez at ca 1700 and 1900 m a.s.l., respectively. Based on pollen analyses and two mid Holocene radiocarbon ages in condensed sections of post-glacial lacustrine and bogs sediments, Chardon (1991) related these two moraines to the Older and Younger Dryas pollen zones, respectively. Two others undated moraine belts are present at around 2500 and 2300 m a.s.l. The higher moraine belt is free of vegetation cover and corresponds to the last advance of glaciers during the LIA (Flusin et al., 1909; Edouard, 1994). These LIA moraines are located on average around 2700 m a.s.l. at less than 100 m below the glacier snout position mapped in AD1977 on topographic maps (Fig. 1C). From the very hot summer in AD2003, however, significant ice melting occurred in the massif. In the catchment area of LBH, this melting induced the formation of a small ice-contact lake at the front of the Rousses glacier and the disappearance of the Herpie glacier (Fig. 1C). Thus, despite its high altitude, LBH constitute one of the few sites in the Alps susceptible to contain a continuous record of Holocene environmental changes because it is located below the LIA moraines and upstream from the Younger Dryas ones.

2.4. Lake-glacier processes

Based on a preliminary multiproxy study of short gravity cores retrieved from LBH and dated by radionuclides activity, Chapron et al. (2007) identified the recent phase of glacier melting and established a conceptual model linking fluctuations of glacier ELAs in the catchment area with observed sedimentary facies since the LIA. This study revealed that enhanced glacier activity (i.e. ELA lowering) in the catchment area resulted in the deposition of dense, magnetic sediments rich in goethite and haematite, but poor in OM (organic matter). Conversely, reduced glacier activity (i.e. ELA elevation) favoured less minerogenic sediment supply to the lake (i.e. fewer occurrences of iron oxides, lower values in magnetic susceptibility and gamma density) and higher content in OM. Chapron et al. (2007) also highlighted that clastic supply to LBH during the melting season was delivered by homopycnal flows developing a steep prodelta in the northern part of the lake (Fig. 2). Sediment failure (Fig. 2) along the slopes of this proximal basin happened in AD1962 due to the regional earthquake of Corrençon (local Richter magnitude ML 5.3) highlighting the sensitivity of LBH to the active seismo-tectonic setting of the Western Alps (cf. Fig. 1A; Thouvenot et al., 2003; Nomade et al., 2005). Superimposed on these sedimentary processes, the occurrence of sedimentary events (SEs) rich in angular dropstones in the lacustrine sediments of LBH were as well related to the impact of frequently observed dirty snow avalanches on the lake-ice in early summer (Chapron et al., 2007).

2.5. Human activities

Human mining activities were detected at high-altitude, 10 km away, between 3770—3870 cal BP (i.e. the Early Bronze Age period) and AD115—330 (i.e. the Roman period) in the northern part of the massif by metallic contaminations in proglacial Lake Bramant (Fig. 1B) varved sediments (Guyard et al., 2007). Mining artefacts were also radiocarbon dated by several archaeological studies (cf. Chapron et al., 2008) at 3800 ± 100 cal BP in the northern part of the massif (Bailly-Maître and Gonon, 2006) and in the south western part of the massif (near LBH lake shore) between 2300 and 1930 cal BP (i.e. the Iron Age) and during the Middle Age between 880 and 665 cal BP (Bailly-Maître and Bruno-Dupraz, 1994). The lead-silver Middle Age mining activity in a vein located few metres from the eastern shore of LBH (Fig. 1C) is also well documented by
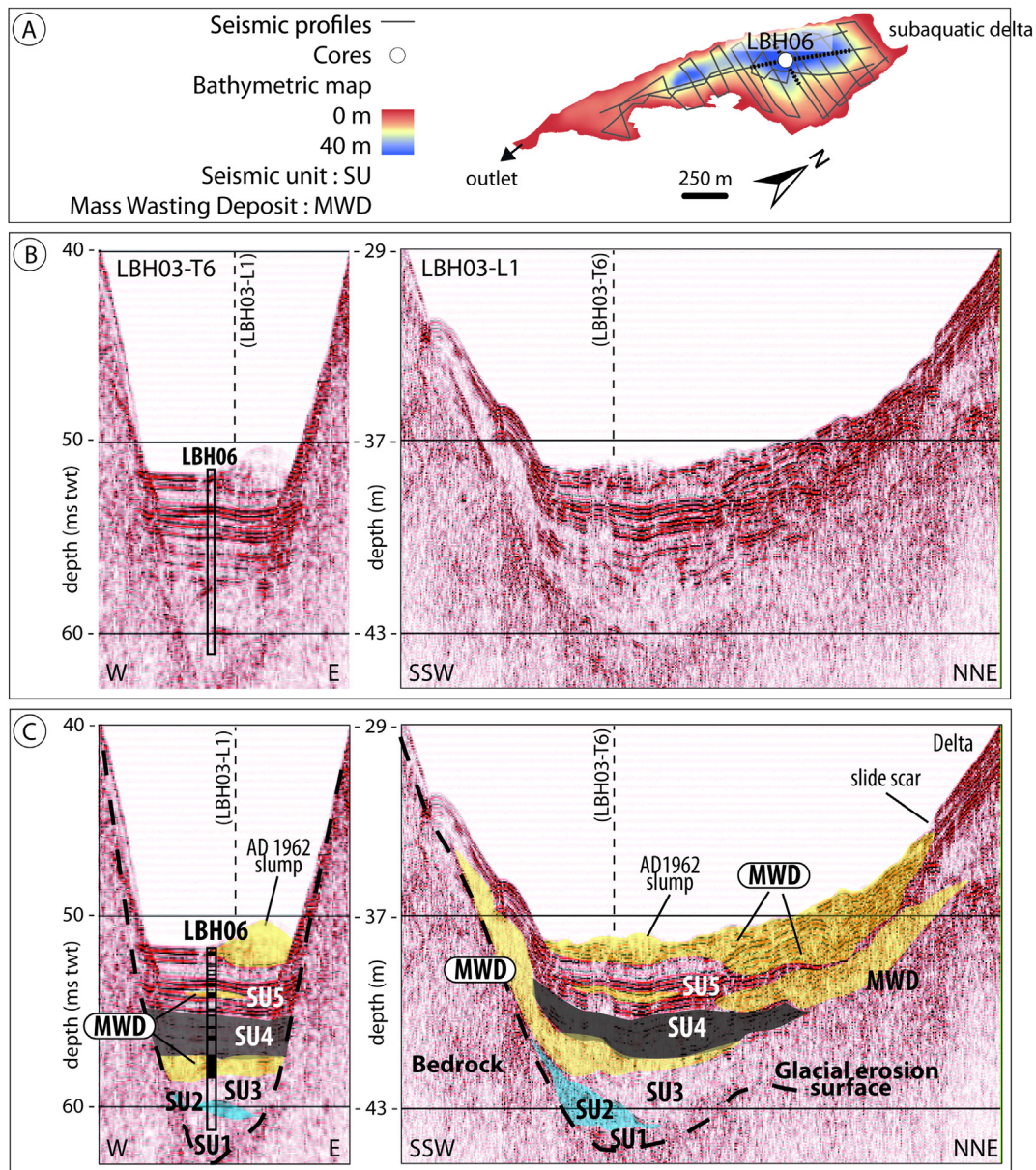
Fig. 2. Location of seismic profiles and sediment core LBH06 in Lake Blanc Huez (A). Illustrations of a transversal (left) and a longitudinal (right) profiles are presented (B) and interpreted (C). These two profiles highlight five seismic units (SU) and the impact of mass wasting deposits (MWD) that are frequently associated with sedimentary events (SE). The latter are shown in black within core LBH06 in (C).

historical chronicles from AD1150 to AD1339: it was exploited along a 120 m-long mineralized fault, and silver ore was extracted using wood fires inside the mine to break the quartz-barite gangue (Bailly-Maître and Bruno-Dupraz, 1994). The silver ore was then separated from the gangue, next to the extraction trench using various techniques (mortar crushing, grindstone grinding, barite calcinations and water washing). During the Roman, period intensive deforestation in the massif is only documented at lower elevations near the Alpe d'Huez ski resort around 2000 m a.s.l. (Fig. 1B, Chardon, 1991).

3. Material and methods

The sedimentary infill of LBH was imaged in September 2003 by high-resolution seismic profiling and partly documented previously in Chapron et al. (2007). A 3.5 kHz pinger system, coupled with GPS navigation, was used from an inflatable boat to record a

dense grid of seismic profiles (Fig. 2). Based on this database, a coring site (LBH06) was selected in the deepest part of the basin, few metres from LBH03 short gravity coring site presented in Chapron et al. (2007), in an area where the infill is the thickest and not largely affected by the AD1962 earthquake triggered slump deposit (Fig. 2).

At site LBH06, sediments were retrieved in February 2006 from the frozen surface of LBH, using an UWITEC piston corer. A pair of overlapping cores were recovered at two nearby locations and allowed the recovery of a 7 m long sedimentary record almost complete: as shown in Fig. 3, a sedimentary hiatus between 434 and 450 cm below the lake floor has been identified once the core sections have been opened, described and correlated based on the identification of key lithological horizons on each core sections.

In June 2008, two non-vegetated soil profiles were sampled in the catchment area of LBH (S1 and S2; Fig. 1C) at 2700 m a.s.l. and 2552 m a.s.l., respectively. Another sample (S3; Fig. 1C) was taken at
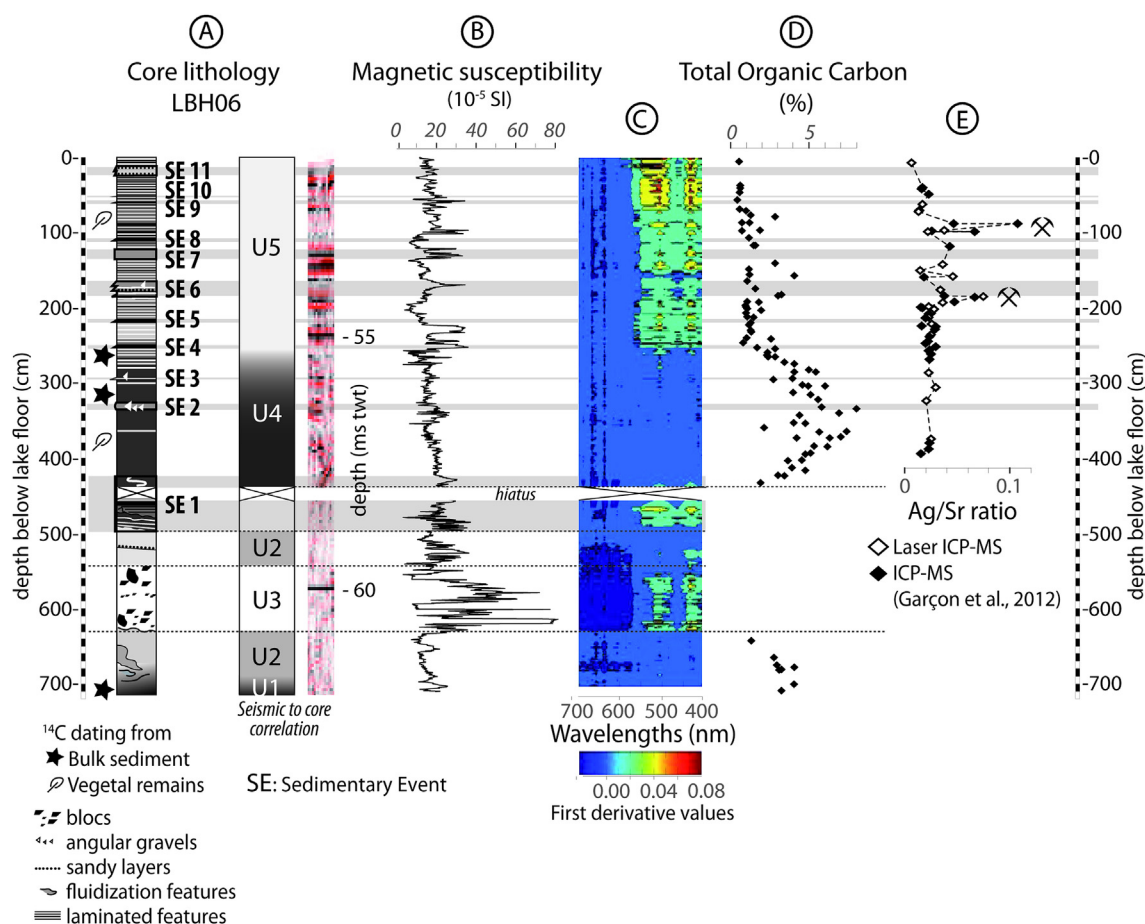
Fig. 3. Core LBH06 (A) is divided into five sedimentary units (from U1 to U5, from base to top). Seismic to sediment core correlation was performed applying a mean P-wave velocity in the sediment of 1500 m s^{-1}. Sedimentary units were defined by variations of the magnetic susceptibility (B), the spectrophotometry (C, here plotted on a 3D diagram where the X axis represent the wavelengths, Y is the depth in core and Z the derivative value for the corresponding wavelength (in nm) expressed by a code of colour), the total organic carbon (D) and the silver on strontium ratio (E, from geochemistry measurements, see the text for more details). (For interpretation of the references to colour in this figure legend, the reader is referred to the web version of this article.)

2084 m a.s.l. outside of the catchment area under typical high-altitude dwarf shrubby vegetation (Poulenard and Podwojewski, 2003). Rocks from the Stefanian coal formation (R, Fig. 1C) were also collected in order to characterize their organic matter signature as described below.

Sedimentological descriptions of LBH06 core lithology (Fig. 3) were supported by digital photographs (Fig. 4) taken at ETH Zurich and laser diffraction grain-size measurements using a Malvern Multisizer 2000 at ENTPE. Additionally, sediment magnetic susceptibility (MS) was measured every 0.5 cm with a Bartington point sensor MS2E and sediment diffuse spectral reflectance measurements were performed every 1 cm using a Minolta CM-700d spectrophotometer following the procedure detailed in Debret et al. (2006). Sediment geochemistry from core LBH03 and LBH06 was analysed by trace element concentrations, measured using a Plasmaquad 2+ ICP-MS, as detailed in Garçon et al. (2012). Additional samples from core LBH06 were also analysed using Laser Ablation ICP-MS, following the procedures described by Gratuze et al. (2001) and Simonneau et al. (2013c).

Rock-Eval (RE) pyrolysis, performed at ISTO, was used to measure the amount of organic carbon in soil, rock and lacustrine sediment samples (Figs. 3 and 5). Total Organic Carbon (TOC, %) and the quantity of hydrocarbon liberated per gram of organic carbon during the pyrolysis stage (the Hydrogen Index, HI) were in particular used to discriminate the specific signature of each

compartment (Copard et al., 2006) from the catchment area of LBH (Fig. 5).

Quantitative organic petrography (QOP) developed by Graz et al. (2010), was also applied to LBH06 lacustrine sediments, soils and rock samples (Fig. 5). Generally, the isolated OM fraction is obtained after the elimination of carbonate and silicate phases by hydrochloric and hydrofluoric acids attacks. This method allows to identify and quantify the major organic constituents (Di Giovanni et al., 1998, 2000; Noël et al., 2001; Sebag et al., 2006; Simonneau et al., 2013a, 2013b, 2013c). Components are characterized by their optical properties (colour and reflectance), their forms (amorphous or figurative) and their origins (algal, phytoclastic or fossil) based on observations with a DMR XP Leica microscope, in transmitted and reflected light modes and with reticule network to determine the surface area of each particle. QOP is improving the conventional palynofacies method introduced by Combaz (1964) and is based on the incorporation of a known mass of a standard (*Cupressus* pollen) in organic concentrate after acid attacks. QOP allows the quantification of organic material inputs into modern environments in mass per gram of sample.

Five radiocarbon dates (AMS) were performed at Poznan radiocarbon laboratory (Poland) from macro remains and bulk sediment sampled in core LBH06, as shown in Figs. 3 and 6, are given in Table 1. Chronology in core LBH06 is established by running the "CLAM" program (Blaauw, 2010) under the mathematic
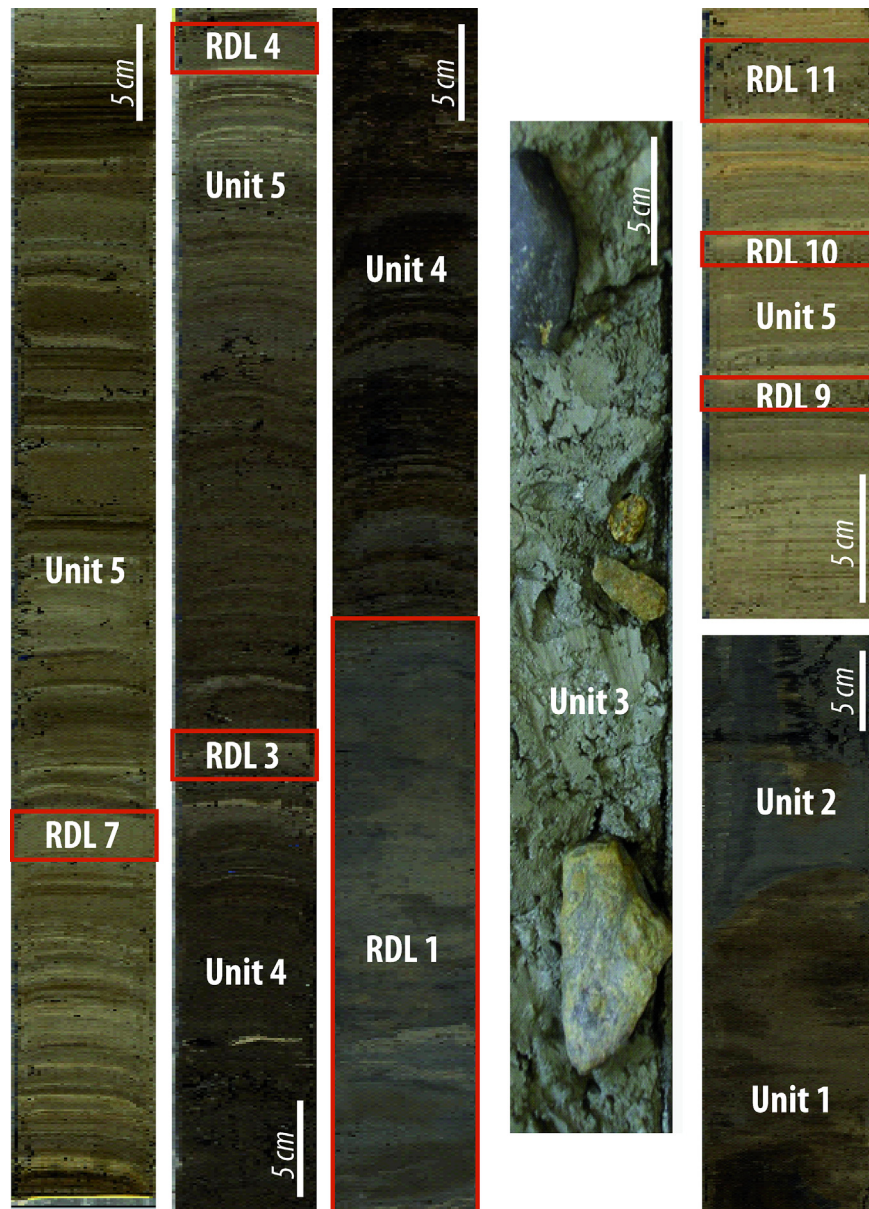
Fig. 4. Photographs illustrating the sedimentary facies described in core LBH06 and associated either with the lithological units numbered from Unit 5 to Unit 1, or with some sedimentary events (SE) delimited by red squares and contrasting with background sediments as detailed in the text. (For interpretation of the references to colour in this figure legend, the reader is referred to the web version of this article.)

software "R" version 2.12.2 based on (i) radiocarbon dates, (ii) the correlation of a recent slump deposit with the AD1962 Corrençon earthquake and (iii) two mining pollution peaks in lacustrine sediments correlated with mining artefacts from the Middle Age and the Iron Age that were radiocarbon dated by Bailly-Maître and Bruno-Dupraz (1994) at the mining archeologistal site next to LBH. The so generated age depth model is additionally supported by the identification of sedimentological evidences of several former regional earthquakes (see below).

4. Results

4.1. Seismic stratigraphy

The seismic signal easily penetrated the relatively thin and locally regularly stratified lacustrine sediments of LBH, but was scattered and absorbed at the acoustic basement, as well as towards the north of the basin, where a steep delta slope exists (Fig. 2). The topography of the acoustic basement and the lake floor bathymetry are characterized by an undulating morphology dividing the lake into three sub-basins on NS longitudinal profiles (Fig. 2). The northern sub-basin is the deepest and highlights the thickest basin fill (ca 10 ms two-way-travel time, twt) on longitudinal profiles. Along West-East transverse profiles, the steep slopes of the lake basin are almost free of sediments and most of the basin fill is occurring in the basin axis. Up to five seismic units (SU) are identified (from base to top) in the northern sub-basin above a high amplitude horizon at the top of the acoustic basement interpreted as an erosion surface (Fig. 2):

SU1 is only occurring in the deepest part of the basin fill, along the axis of the basin and its limits are not well defined. This thin unit is characterized by a transparent acoustic facies. SU2 is
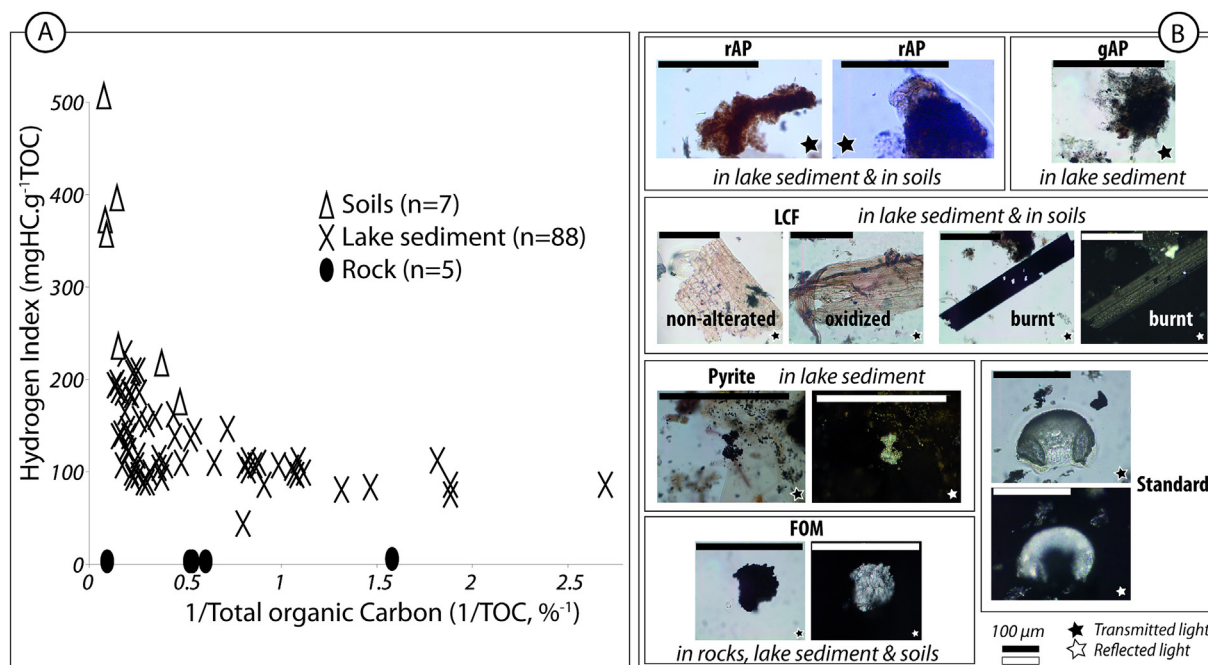
Fig. 5. Rock-Eval pyrolysis results (A) are represented on a Hydrogen Index *versus* 1/Total Organic Carbon diagram for soil (white triangles), lake sediment (black crosses) and rocks (black dots) samples. The main constituents of the organic fraction identified and quantified by quantitative organic petrography are represented (B). Rock samples are only composed of fossil organic matter debris (FOM). Red Amorphous Particles (rAP), Ligno-Cellulosic Fragments (LCF) and FOM are found in soil and lacustrine samples whereas grey Amorphous Particles (gAP) and pyrite are only found in lacustrine samples. (For interpretation of the references to colour in this figure legend, the reader is referred to the web version of this article.)

essentially occurring along the axis of the basin and is locally producing discontinuous high amplitude reflections together with hyperbolae. SU3 is thicker and occurring in most of the deep lake basin. It is characterized by a transparent acoustic facies. SU4 is producing a transparent acoustic facies with several sub-horizontal low amplitude and discontinuous reflections laterally onlaping at the contact with the acoustic substratum. SU5 is the thickest unit and is made of laterally continuous sub-parallel high-amplitude reflections characterized by a draping pattern. SU5 thins towards the South and develops onlaps at the contact with the acoustic substratum.

In addition to these seismic units, several lens-shaped transparent bodies of variable size with rare chaotic internal reflections of variable amplitudes are occurring within SU5 (close to the lake floor and along the slopes of the delta) and in between SU3 and SU4 (Fig. 2C).

4.2. Core lithology and sediment compounds

Up to five sedimentary units and eleven sedimentary events (SEs) can be identified (from base to top) within the 713-cm-long core LBH06 based on a multiparameter approach (Figs. 3 and 4):

Unit 1 (U1, from 713 to 695 cm core depth) is a sandy silt dark to brownish deposit locally highlighting some folded bedding and characterized by low MS values ($\sim 18 \cdot 10^{-5}$ SI) but relatively high TOC content (4%).

Unit 2 (U2, from 695 to 630 cm and from 540 to 490 cm) is a sandy silt light grey deposit characterized by fluctuations of MS values (from 15 to $30 \cdot 10^{-5}$ SI) and decreasing TOC content from base to top (from 4 to 1.5%).

Unit 3 (U3, from 630 to 540 cm) is composed of a light grey silty and compact matrix containing numerous coarse to very coarse angular gravels and very small boulders (7 cm) according to the classification of Wentworth (1922) of variable compositions. This unit, defined by high MS values ($>20 \cdot 10^{-5}$ SI) and two sharp

reflectance peaks culminating at 445 and 525 nm, respectively (Fig. 3C), occurs above an erosive surface.

SE 1 (from 490 to 421 cm) is a dark to light grey deposit developing a mottled pattern locally bearing fluidization features and several pluri-centimetric sections characterized by sub-parallel and tilted laminations. These sediments have fluctuating MS values (from 0 to $35 \cdot 10^{-5}$ SI) and two main reflectance peaks at 445 and 525 nm. A hiatus due to coring operations also occurred within SE 1 between 450 and 434 cm.

Unit 4 (U4, from 421 to 280 cm) is a black to dark grey silty sand deposit containing few pluri-millimetric to centimetric light grey laminas. These sediments have low MS values ($15 \cdot 10^{-5}$ SI), high TOC content ($>4.5\%$) and low values of the Ag/Sr ratio (0.02). U4 is occurring above SE 1 and is locally interrupted by SE 2 (5 cm thick) and SE 3 (1 cm thick) at 330 and 295 cm core depth, respectively. These two layers have higher MS values and have coarser granulometry than unit 4. They are also characterized by the occurrence of few pebbles and gravels with angular morphologies.

The transition between units U4 and U5 is gradual (from 280 to 260 cm) and marked by enhanced fluctuations of MS values, by a progressive decrease in TOC content (from 4 to 1%), and by a progressive occurrence of reflectance peaks at 445 and 525 nm.

Unit 5 (U5, from 260 to 0 cm) consists of light grey finely laminated sandy silts characterized by MS values fluctuating around $20 \cdot 10^{-5}$ SI, relatively low TOC content (between 0.5 and 4.5%), two reflectance peaks (at 445 and 525 nm) and two outstanding peaks of the Ag/Sr ratio at 90 and 185 cm core depth. Up to eight SEs (SE 4–11) are identified within U5: SE 4, 5, 7, 8, 9, 10 and 11 are centimetric brownish sandy deposits with a sharp basal contact and a graded base fining upward. They are also characterized by relative peaks in MS values (excepted SE 5 and 11). SE 6 is the thickest unit of this kind (18 cm thick) and is characterized by fluctuating MS values, several sandy beds and few pebbles and gravels with angular morphologies.
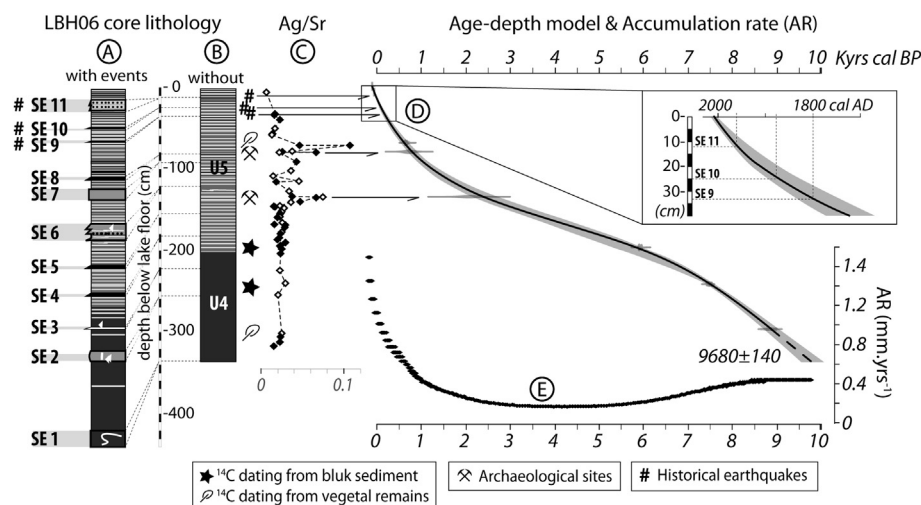
Fig. 6. Age-depth model of core LBH06 based on the identification of sedimentary events (SE) on the core lithology (A) that have been removed in the synthetic core lithology (B). Four radiocarbon ages, performed on vegetal remains (white leaves) or bulk samples (black stars) and the identification of two phases of human mining activities here highlighted by two Ag/Sr peaks (C) were used to establish the chronology. Age-depth model (D) and the associated accumulation rate (E) were obtained running a clam model (Blaauw, 2010).

RE analyses, represented here by the graph "Hydrogen Index (HI) *versus* 1/TOC" (Fig. 5A), indicate that the organic matter from geological formation (i.e. coal rocks, "R" sample, Fig. 1C), soils ("S1, S2, S3" samples, Fig. 1C) and lacustrine samples (core LBH06, Fig. 1C) have contrasted signatures. Coal formation is characterized by a high degree of thermal maturity (Tmax = 487 °C), HI inferior to 2 mgHC g^{-1} TOC, corresponding to altered material, and variable organic contents (10 > TOC > 0.6%). Soils (Fig. 5A) are defined by a lower degree of thermal maturity (Tmax < 400 °C). Superficial soil layers are described by HI superior to 300 mgHC g^{-1} TOC, typical of non-altered terrestrial debris (Sebag et al., 2005) and high organic content (TOC > 10%), while deeper soil layers are defined both by lower HI values (around 200 mgHC g^{-1} TOC), typical of the terrestrial pole (Simonneau et al., 2013b) and a lower TOC (7 > TOC > 2%). Lacustrine sediments have also a low degree of thermal maturity (Tmax < 400 °C) but are characterized by inter-mediate values both of HI (fluctuating between 43 and 195 mgHC g^{-1} TOC), that is between the soil and the coal formation domains (Fig. 5A) and a variable TOC ranging between 8 and 0.4%.

In addition to the standard added in sample preparation (*C. pollen*), QOP analyses revealed twelve types of organic particles presented in Fig. 5B. Coal formation samples are exclusively composed of squat opaque particles with very high reflectance similar to the ones described by Graz et al. (2011) and correlated to fossil organic matter debris (FOM, Fig. 5B). Soils contain some of these FOM particles but also numerous palynomorphs (i.e. pollens and spores) and non-palynomorphs microfossils, such as ligno-cellulosic fragments (TLC, Fig. 5B) with different aspects depend-ing of their degree of alteration (from non-altered to burnt par-ticles defined by irregular boundaries and internal small dark vesicles observed in reflected light) and red colloidal amorphous

particles with diffuse limits and no internal structure (rAP, Fig. 5B). All lacustrine sediment samples only differ from the watershed ones by the presence of grey amorphous particles (gAP, Fig. 5B) corresponding to product of algal growth in the lake waters (Patience et al., 1995; Simonneau et al., 2013a, 2013b, 2013c) and rhombohedral pyrite suggesting some periods of anoxic conditions, in particular throughout the sedimentary unit U4.

4.3. Radiocarbon dating

The five AMS radiocarbon dates from LBH06 (Table 1) indicate that the sedimentary units U5 and U4 cover most of the Holocene period and that the sedimentary unit U1 corresponds to the end of the Lateglacial period. QOP analyses of bulk sediment samples dated by radiocarbon in sedimentary units U1 and U4 suggest, however, that the occurrence of FOM is affecting the age calculation (Graz, 2009). As described below (see Section 5.2), a correction has been applied to radiocarbon ages obtained from bulk sediment samples in LBH06.

5. Interpretations and discussions

5.1. LBH basin fill evolution

The seismic stratigraphy of LBH basin troughed by core LBH06 together with the geological setting and the composition of soil samples in this part of the Grandes Rousses Massif allow doc-umenting the general evolution of the basin fill of this proglacial lake and identifying the main sources of lacustrine sediments.

The erosion surface identified at the base of the sedimentary infill of LBH on seismic profiles forms three narrow and over

Table 1
Radiocarbon dates obtained from core LBH06. Age calibration was done using sets by Reimer et al. (2009).

Materiel dated	Laboratory	Initial depth (cm)	Corrected depth (cm)	Initial radiocarbon date (BP)	Fossil organic matter quantified by quantitative organic petrography (%)	Corrected radiocarbon date (BP)	Calibrated radiocarbon ages (cal BP)
Wood debris	Poz-18873	87	69	774 ± 50	—	—	725 ± 65
Bulk	Poz-29439	265	197	5250 ± 35	0.8	5185 ± 35	5950 ± 55
Bulk	Poz-18874	312	242	6770 ± 40	2.08	6600 ± 40	7480 ± 45
Wood debris	Poz-18875	372	297	8000 ± 50	—	—	8855 ± 155
Bulk	Poz-18877	703	—	11 240 ± 80	8.71	10 510 ± 80	12 370 ± 235

deepened sub-basins delimited by bedrock sills which is typical from glacier erosion (Moscariello et al., 1998; van Rensbergen et al., 1999; Chapron et al., 2007; Fiore et al., 2011). Based on available chronologies in quaternary formations from this massif (Chardon, 1991), this erosion surface can be related to the last glaciation.

Above this erosion surface, the upper part of seismic unit SU1 has been sampled at the base of core LBH06 and can be correlated to the fined grained sedimentary units U1 and U2. The organic rich sedimentary unit U1 which is mainly composed of gAP and characterized by high IH values, illustrate the predominance of algal particles and can thus be interpreted as gyttja deposits (Hansen, 1959; Talbot and Livingston, 1989; Simonneau et al., in press). Following Dahl et al. (2003), this suggests that glaciers were no longer present in the watershed anymore when these autochthonous lacustrine sediments were deposited. Conversely, the drop of TOC and fluctuating values of sediment MS in sedimentary unit U2 (occurring below and above sedimentary unit U3), is interpreted as resulting from significant glacier development upstream from LBH (Fig. 3). This hypothesis is strongly supported by the correlation of sedimentary unit U3 with seismic unit SU2 (Fig. 2), where the identification of high-amplitude hyperbolas can be related to the occurrence of rather large rock debris mixed into a compacted fine-grained sedimentary matrix, a typical signature of subaqueous moraine deposits (Moscariello et al., 1998; Fiore et al., 2011). The compacted matrix of sedimentary unit U3 is, in addition, dominated by two reflectance peaks centred on 445 and 525 nm (Fig. 3), reflecting the occurrence of oxyhydroxyde goethite in the sediments (Deaton and Balsam, 1991; Debret et al., 2006). This can therefore be related to significant bedrock erosion by glaciers in the catchment area of LBH as previously proposed by Chapron et al. (2007). Sedimentary unit U3 indicates also that the glacier grounding base was close to LBH06 coring site during this period. The two occurrences of sedimentary unit U2 can therefore be interpreted as glaciolacustrine deposits accumulated in front of the glacier during its last major development in LBH basin.

The large lense-shaped body with chaotic internal reflections of variable amplitudes identified in between seismic units SU3 and SU4 (Fig. 2C) has been sampled in LBH06 and corresponds to SE 1, which is composed of a mixture of organic and minerogenic lacustrine sediments has reflected by fluctuating MS values and the occurrence locally of goethite highlighted by two reflectance peaks centred around 445 and 525 nm (Fig. 3). The acoustic signature of this deposit together with the successive sedimentary facies identified on core are typical of a subaqueous mass wasting deposit (MWD, Fig. 2) in clastic alpine lakes having steep slopes (Chapron et al., 2004; Schnellmann et al., 2006; Fanetti et al., 2008; Lauterbach et al., 2012). This MWD is identified along the southern slope and in the axis of the main sub-basin where it thins toward the North (Fig. 2), suggesting that its main sediment source was originating from the southern slope of the basin.

The overlying seismic unit SU4 corresponds to the organic rich sedimentary unit U4 which is mainly composed of algal particles and thereby interpreted as a gyttja. This sedimentary facies therefore reflects the disappearance of glaciers in the watershed of LBH. The occurrence of two low-amplitude and discontinuous reflections within seismic unit 4 can in addition be correlated to the deposition of SE 2 and 3. Following Seierstad et al. (2002) and Chapron et al. (2007) these coarser layers, composed of frequent angular rock debris, are interpreted as dirty snow avalanche deposits accumulated on the frozen lake and reached the lake floor once the lake ice started to break and melt.

The uppermost seismic unit SU5 is correlated to the minerogenic sedimentary unit U5, rich in goethite but also showing variable values of TOC and sediment MS (Figs. 2 and 3). This unit is in addition developing a steep lacustrine prodelta geometry in the

northern part of the subbasin suggesting that sedimentation is here dominated by homopycnal and hyperpycnal flows (Chapron et al., 2007, 2009; Mulder and Chapron, 2011). These characteristics are reflecting a growing and fluctuating influence of glacier activity in the catchment area on proglacial lacustrine sedimentation. Several MWDs with chaotic internal reflections of variable amplitudes (Fig. 2B and C) are also identified on seismic profiles close to the lake floor and along the slopes of the delta where they are generally the thickest. This suggest that these MWDs where essentially initiated along the slopes of the delta. The uppermost MWD is in particular associated with a fresh slide scar in the prodelta and remoulded large volumes of sediments in the northern sub-basin. This deposit has been sampled by gravity cores, dated and interpreted by Chapron et al. (2007) as a slump deposit triggered by the AD1962 Corrençon regional earthquake. In core LBH06, this historical event is correlated to the uppermost SE11 and interpreted as a distal deposit due to a MWD. The other SEs identified within this unit in core LBH06 are characterized by coarser grain size than the background sediments and may be responsible for the development of continuous higher amplitude reflections within this seismic unit, excepted the thickest one (SE 6) which can be correlated with a lense-shaped MWD identified in the axis of the basin (Fig. 2B and C).

5.2. Chronology of core LBH06

5.2.1. AMS ^{14}C dating on bulk samples

Graz (2009) demonstrated that the presence of fossil organic matter (FOM) can make older AMS ^{14}C dating on bulk material. The occurrence of FOM in LBH06 sediments can only be explained by erosion (glacier abrasion; weathering, snow avalanches, etc…) of the Stefanian coal formation outcropping along the eastern part of LBH catchment area and presently partly covered by the Rousses glacier (Fig. 1). Because the coal formation is only made of squat opaque particles, they are considered as specific organic tracers. Their quantification in lacustrine samples from core LBH06 can be used to correct AMS dates on bulk sediment samples since ageing is proportional to coal percentage in the bulk material (Graz, 2009). Adapting the radioactive decay low of Libby (1967) and quantifying coal richness by QOP, we calculated radiocarbon ages corrections for bulk samples Poz-29439, Poz-18874 and Poz-18877 and estimated them at 65, 170 and 730 years, respectively (Table 1). These corrections should thus be subtracted to the initial radiocarbon age before being calibrated and used in the age-depth model.

5.2.2. Archaeological data

Following Garçon et al. (2012), the Ag/Sr ratio in core LBH06 can be used to track the evolution of runoff pollutions originating from mining activities in the lead–silver vein located close to the eastern shore of LBH (Fig. 1C). Fig. 6 illustrates the evolution the Ag/Sr ratio in the sedimentary units U5 and U4 from core LBH06 without SEs and highlights three outstanding peaks within U5 corresponding to two phases of mining exploitation. The first outstanding peak in Ag/Sr identified in older sediments at 135 cm (corrected depth, Fig. 6) can be related to mining activities documented by Bailly-Maître and Bruno-Dupraz (1994) during the Iron Age, based on a radiocarbon date (2115 ± 185 cal BP) from wood charcoals sampled at the archaeological site. The two more recent outstanding peaks suggest one bipartite phase. The highest value of the Ag/Sr ratio is contemporaneous to a radiocarbon date (720 ± 70 cal BP; AD1220 ± 70) obtained from wood debris in LBH06. This peak can therefore be related to the Middle Age mine that has been well-documented at the lake shore between AD1150 and AD1339 by Bailly-Maître and Bruno-Dupraz (1994). The lower value of the secondary peak in Ag/Sr ratio identified just below is thus

interpreted as the beginning of the resumption of mining activities around LBH. It can be related to 770 ± 100 cal BP based on the radiocarbon age obtained from wood pillars at the Middle Age mining site and previously published by Bailly-Maître and Bruno-Dupraz (1994).

5.2.3. LBH06 age-depth model

The corrected radiocarbon age of 12 370 ± 240 year cal BP from bulk sediments of unit U1 at the base of core LBH06 is in agreement with the conclusions of Chardon (1991) suggesting that the Grandes Rousses massif deglaciation started before the Lateglacial—Holocene transition.

The age model of sedimentary units U4 and U5 in core LBH06 was computed using a smooth spline function (Blaauw, 2010) and reported on Fig. 6. It is covering most of the Holocene and is established based (i) on a corrected composite depth with the thickness of the SEs being subtracted (Fig. 6B), since these event layers correspond to instantaneous events (cf. Lauterbach et al., 2012) and (ii) on eight chronological markers: two AMS ^{14}C dates on macroremains, three AMS ^{14}C dates on bulk sediment corrected from the occurrence of fossil organic matter, two radiocarbon dates from the nearby archaeological site correlated with Ag/Sr peaks tracking former local mining activities, and the stratigraphic correlation of SE 11 with the slump deposit from core LBH03 dated by radionuclide and related to the impact of the AD1962 Corrençon earthquake located at 47 km from LBH (Chapron et al., 2007). LBH06 constitute therefore a continuous sedimentary record of environmental changes at high-altitude in the western French Alps since 9680 ± 140 cal BP and is characterized by a progressive change in sedimentation during the Late-Mid Holocene transition from the organic rich unit U4 toward a more clastic unit U5. A progressive drop in sedimentation rate from 0.4 to 0.2 mm yrs^{-1} is identified during this major change in sedimentation, while over the last 2000 years, sedimentation rate exponentially increased from 0.25 to 1.4 mm yrs^{-1} (Fig. 6E). Based on visual observations, higher water content in recent sediments covering the last 2000 years might partly explain such a significant increase of sedimentation rate. This recent sedimentation rate is, however, strongly supported by the correlation of 3 sedimentary events (SE) with historical regional earthquakes (Fig. 6D, Table 2).

This age model (Fig. 6D) allows estimating the chronology of SEs (Table 2) and is comforted by the correlation of SE 10 with the AD1881 Allemond earthquake (Nomade et al., 2005; Guyard et al., 2007; Wilhelm et al., 2011) located at 6 km from LBH and SE 9 either with the largest regional earthquake located next to Lake Le Bourget at 80 km from LBH in AD1822 (the Chautagne event, Chapron et al., 1999; Guyard et al., 2007), or with a smaller but local event in AD1782 (the Uriage earthquake; Nomade et al., 2005; Wilhelm et al., 2011) located at 20 km from LBH (Fig. 1B). Similarly, SE 1 is, within the age-depth models errors, synchronous, with a major subaquatic slope failure event (the HDU) in Lake Le Bourget dated between 9400 and 9700 cal BP and attributed to a large paleo-earthquake (Chapron et al., 1996, 2004; van Rensbergen et al., 1999; Debret et al., 2010; Arnaud et al., 2012). Following the classification of Mulder and Cochonat (1996), SE 1 and SE 11 are interpreted as slide deposits, while SE 9 and SE 10 are graded beds typical from thin distal turbidites. This is suggesting that these MWDs (i.e. mass wasting deposit) in LBH are resulting from earthquake-induced subaquatic slope failures and can be considered as natural archives of former regional earthquakes in this part of the Alps. Similarly, the others subaquatic MWDs from LBH06, labelled SE 4, 5, 7 and 8, might correspond to previously undocumented (and eventually more local) earthquakes around 5400, 3700, 1150 and 650 cal BP. Following Chapron et al. (2007), SE 2, 3 and 6 are related to avalanche deposits since they contain angular

Table 2
Estimated ages and characteristics of the sedimentary events (SEs) recorded in LBH06 and discussed in the text.

Sedimentary events identified in LBH06	Estimated ages	Triggered mechanisms	Related regional events
SE11	AD1960 ± 4	Historical earthquake	AD1962 Corrençon earthquake
SE10	AD1870 ± 11		AD1881 Allemond earthquake
SE9	AD1800 ± 2		AD1822 Chautagne earthquake AD1782 Uriage earthquake
SE8	675 ± 55 cal BP	Palaeo-earthquake?	
SE7	1135 ± 125 cal BP		
SE6	2155 ± 235 cal BP	Avalanche	
SE5	3685 ± 240 cal BP	Palaeo-earthquake?	
SE4	5375 ± 175 cal BP		
SE3	6980 ± 90 cal BP	Avalanche	
SE2	7250 ± 70 cal BP		
SE1	9680 ± 140	Palaeo-earthquake	Lake Le Bourget HDU (9550 ± 150 cal BP)

rock debris and suggest that LBH was not significantly exposed to this type of natural hazards during the Holocene.

5.3. Holocene high-altitude environmental changes

5.3.1. Glacier fluctuations

Following Dahl et al. (2003), the identification of organic rich sediments at the base of core LBH06 clearly indicate that Rousses and Herpie glaciers were much reduced in the drainage basin of this proglacial lake around 12 400 cal BP. The deposition of glacio-lacustrine sediments (sedimentary unit U2) and the formation of a subaquatic moraine (sedimentary unit U3) before the onset of gyttja accumulation during the Boreal period (sedimentary unit 4) suggest that the last important growing of Rousses and Herpie glaciers (at least down to 2550 m a.s.l.) took place either during the Younger Dryas or the Preboreal periods. This last most extended glacier advance in the Grandes Rousses Massif might therefore match the Egesen maximum documented in the Swiss and Austrian Alps by Ivy-Ochs et al. (2009) and dated around 12 200 ± 1000 cal BP by ^{10}Be.

Based on the application of Chapron et al. (2007) conceptual model linking LBH sedimentation pattern with glacier activity and ELA fluctuations in its catchment area, the following Holocene period can be divided in two contrasting units and stages (Figs. 3 and 7): a first period characterized by very limited to absent glaciers from the Early to the Mid Holocene reflected by high values of TOC (Fig. 7A) but lower ones of oxyhydroxyde goethite (Fig. 7C) within the sedimentary unit U4, contrasting with a second period covering the last ca 5000 years, when glaciers were much more developed, as shown by lower TOC values (Fig. 7A) and higher goethite contents (Fig. 7C) measured within the sedimentary unit U5. Between ca 1800 and 1600 cal BP (ca AD150 ± 200 and AD350 ± 200), according to the resolution of the age-depth model (Fig. 6), an abrupt increase of TOC and a drop of goethite are, however, reflecting a short episode of very limited glaciers activity during the Roman period (Fig. 7).

This general pattern during the Holocene is in addition strongly supported by the simultaneous enrichment of FOM (Fig. 7H) and the lowering of sediment mean grain size (Fig. 7F) in LBH06 between ca 5000–1800 cal BP and since ca 1600 cal BP. Both proxies reflecting respectively: (i) enhanced glacier abrasion of the
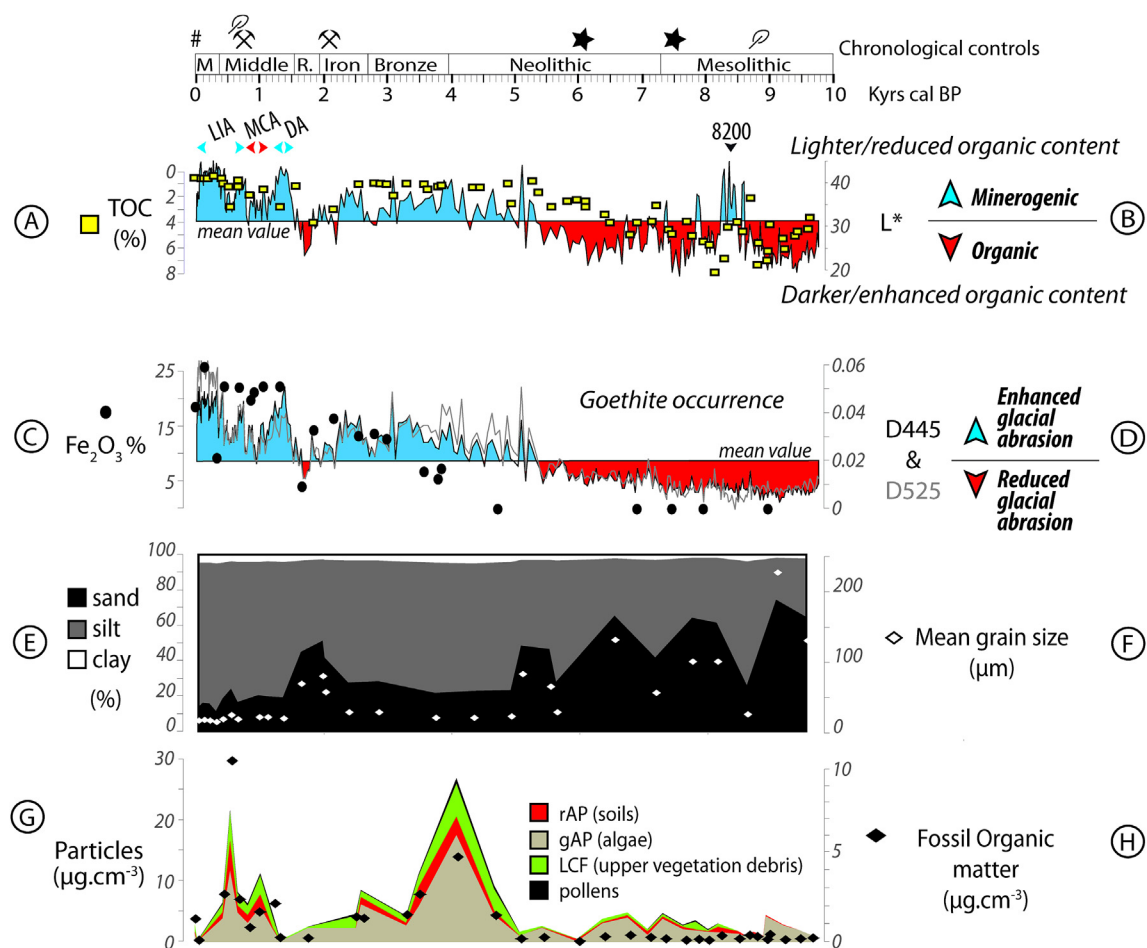
Fig. 7. Detailed sedimentology of core LBH06 without event layers. Total Organic Carbon values (A) are anti-correlated to L* fluctuations given by spectrophotometry (B). Iron oxides contents given by laser-ICPMS measurements (C) are correlated to fluctuations of the two derivatives D445 and D525 given by spectrophotometry (D). Finally, grain size analyses are plotted (E and F) and the results of quantitative organic petrography are also represented (G and H). Symbols used for chronological markers are the same than the ones used in Fig. 6.

Stefanian coal formation at the head of the drainage basin (cf. Fig. 1) and (ii) enhanced amount of silt- and clay-size particles originating from glacial abrasion and transported in suspension by glacial melt waters before being deposited in LBH. The transition from unit U4 to U5 in LBH can therefore be related to the onset of the Neoglacial period in the western French Alps ca 5400 cal BP.

High-resolution measurements of LBH06 sediment diffuse spectral reflectance such as lightness (L*, Fig. 7B) and derivatives 445 nm and 525 nm (Fig. 7D) being significantly correlated with TOC (Fig. 7A, $R = -0.72$, $p < 0.01$) and Fe_2O_3 (Fig. 7C, $R = 0.61$, $p = 0.007$ for D445; $R = 0.65$, $p = 0.015$ for D525) contents, respectively, it is also possible to further document the variability of glacier activity at a centennial time-scale during the Holocene.

Over the last 2000 years, when our age-depth model is best constrained (Fig. 6), lighter sediment (i.e. enhanced minerogenic content) and high content in oxyhydroxide goethite (i.e. enhanced glacial abrasion) are highlighting in particular the bipartition of the Little Ice Age with a first phase of enhanced glacier activities between AD1160 ± 130 and AD1275 ± 55 (i.e. 675 ± 130 and 785 ± 55 cal BP) and a last phase when glacier activity culminated between AD1500 ± 50 and AD1917 ± 10 (i.e. 450 ± 50 and 33 ± 10 cal BP) in agreement with Flusin et al. (1909) observations and Chapron et al. (2007) reconstructions. Interestingly, a similar outstanding peak in glacier activity is evidenced during the Dark Age period between AD415 ± 135 and AD760 ± 180 (i.e. 1190 ± 135

and 1535 ± 180 cal BP). It is strongly contrasting with a minimum of glacier activity during the Roman period when both spectrophotometric parameters are below the mean values calculated for the sedimentary units U4 and U5 (Fig. 7). Fluctuating and moderate glaciers activity is also detected during the Medieval Climate Anomaly between AD760 ± 135 and AD1160 ± 130 (i.e. 1190 ± 135 and 790 ± 130 cal BP) and the Iron Age (between 2150 ± 230 and 2220 ± 240 cal BP). A similar limited and oscillating glacier activity is in addition suggested during the Bronze Age period and since the second part of the Neolithic period, i.e. during the beginning of the Neoglacial period. Limited chronological controls during these time windows in core LBH06 is however currently preventing any further detailed environmental reconstructions for this part of the Grandes Rousses Massif, but rapid glacier fluctuations are well-documented by Guyard et al. (2007) in the northern part of the massif, based on the identification organic-rich annually laminated proglacial sediments from Lake Bramant (Fig. 1B) during the Bronze Age (i.e. between 4160–3600 and 3300–2850 cal BP). These interpretations from the sedimentary record of LBH are also in agreement with the identification of several phases in the Alps (i) of reduced glacier activity during the Late Neolithic and the Roman period and during the Iron and Medieval Climate Anomaly (Holzhauser and Zumbühl, 1999; Hormes et al., 2001; Deline and Orombelli, 2005; Holzhauser et al., 2005; Debret et al., 2010) and (ii) of enhanced glacier activity since the onset of the Neoglacial, at

the beginning of the Iron Age and later during the Dark Ages and the Little Ice Age (Leeman and Niessen, 1994; Chapron et al., 2005, 2008; Deline and Orombelli, 2005; Holzhauser et al., 2005; Vincent et al., 2005; Guyard et al., 2007; Wanner et al., 2008; Debret et al., 2010).

5.3.2. Soil erosion

Holocene organic matter from lacustrine sediments of LBH is essentially composed of grey amorphous particles (gAP, Fig. 7G) resulting from algal productivity in the water column. Following Reynolds et al. (2000), this means that both lake waters temperature, oxygen content, transparency and nutrients loading remained favourable and promoted phytoplankton production during this interglacial period. Phases of enhanced algal production are however identified around 4000, 2500, 1000 and 500 cal BP (Fig. 7G) and suggest that some of the above mentioned lake waters parameters were significantly fluctuating during the Late Holocene.

Other primary source of organic material in lake sediments such as plant detritus, pollen, soil or fossil organic matter (Meyers and Ishiwatari, 1993; Graz et al., 2010) are also variable in LBH06 during the Holocene and may thus provide key additional evidences for environmental reconstructions. As previously mentioned, FOM in LBH06 can only result from glacier abrasion, weathering and snow avalanching affecting the Stefanian coal formation outcropping at the head of the drainage basin (Fig. 1C). The occurrence of FOM in background sediments from LBH06 (i.e. not in SEs) documented in Fig. 7G is thus interpreted as a proxy for runoff processes at the head of LBH drainage basin during the first part of the Holocene (i.e. when glacier activity was very limited). Since the onset of the Neoglacial period, the occurrence of FOM in LBH06 is probably mainly linked to glacier abrasion but the contribution of runoff cannot be excluded.

Pollens recorded in high-altitude sites usually come from lower altitudes ones after being lifted by vertical air-mass movements (Talon, 2010) and are thus only providing a very general and regional picture of the vegetation cover in surroundings mountainous environments. On the contrary, LCF (Fig. 7G) quantified throughout the lacustrine sediment in LBH06 are similar to the ones described in the present-day soils samples S1 and S2 from the LBH watershed and soil sample S3 taken nearby under a typical high altitude dwarf shrubby vegetation (Fig. 1C). LCF can therefore be here related to upper vegetation debris inherited from the original vascular plant, such as grasses or shrubs. Similarly, the rAP (Fig. 7G) are common in core LBH06 and in the present-day soils samples S1, S2 and S3. They are also similar to the ones observed in soil and lacustrine environments from contrasted environments by Noël et al. (2001); Sebag et al. (2006) or Simonneau et al. (2013a, 2013b, in press) and are thus correlated to paedological processes in the drainage basin of LBH. Consequently, the occurrence of paedological markers together with upper vegetation debris in the lacustrine sediments of LBH can be interpreted as resulting from the erosion over the Holocene by runoff processes of a sporadic emergent vegetation (Meyers and Ishiwatari, 1993) possibly similar to the present-day cover in the drainage basin of LBH. This suggests that the treeline position remained below 2550 m a.s.l. in this part of the Grandes Rousses massif over the Holocene, in agreement with the conclusions of Carnelli et al. (2004) and Talon (2010) estimating that the elevation of the timberline were around 2500 m a.s.l. during the Early Holocene in central European Alps and French Southern Alps, respectively.

The occurrence of soil particles in LBH06 (Figs. 7G and 8B) indicates that paedological layers (Leptosols, cf. IUSS, 2006 and Burga et al., 2010) were developed since ca 12 300 years above 2550 m a.s.l. Such steep and grassy slopes are prone to soils erosion

and exportation within the drainage basin by runoff processes (Graz et al., 2010), especially when submitted to snowmelt erosion (Ollesch et al., 2006; Tanasienko et al., 2009, 2011). Phases of enhanced soils particles content in LBH06 identified at 8500–8000 cal BP, 7500–6800 cal BP, 4500 and 2500 cal BP and finely between 1200 and 400 cal BP (Fig. 8A), are thus interpreted as resulting from enhanced runoff processes along the steep and grassy slopes of LBH drainage basin which were largely submitted to snowmelt.

The first significant occurrence of soil erosion from ca 8500 to 6800 cal BP (Fig. 7G) is also matching higher values of L* in LBH06 (Fig. 7B) reflecting higher clastic supply to LBH. Since glaciers were very limited during the Early Holocene, this signal is interpreted as resulting from relatively colder and wetter conditions at high-altitudes before the onset of the Neoglacial. This signal could partly reflect: (i) the impact of the 8.2 event documented in the northern hemisphere (Alley et al., 1997; Alley and Agustsdottir, 2005; Lajeunesse and St-Onge, 2008) and around the Alps (von Grafenstein et al., 1999) and (ii) other humid and cooling abrupt phases also identified in the Alpine realm at lower altitudes based on pollen assemblages, lake levels and large alpine rivers flooding activity (Haas et al., 1998; Magny, 2004; Debret et al., 2010).

Enhanced soil erosion between ca 4500 and 2500 cal BP is similarly interpreted as resulting from more pronounced snowmelt erosion within the drainage basin of LBH and is highlighting a progressive development of colder and wetter conditions after the onset of the Neoglacial period. Such a climate change at high altitude favoured the development of glaciers at the head of the catchment area as reflected by the increasing content of goethite and FOM in LBH06 (Figs. 7 and 8). During this period, several more humid and cooler phases were also identified in the Alps by vegetation, glacier and paleohydrological reconstructions based on well-dated sedimentary archives (Haas et al., 1998; Magny, 2004; Vollweiler et al., 2006; Guyard et al., 2007, 2013; Debret et al., 2010).

Between ca 1200 and 400 cal BP, enhanced snowmelt erosion and higher runoff are also identified by the amount of rAP in core LBH06 (Fig. 7G) and suggest contrasting prevailing temperature and precipitation conditions at high-altitude especially during the first part of the LIA (around AD1400 ± 50) and during the Medieval Climate Anomaly (around AD890 ± 115). The highest values of soil erosion during the LIA is in agreement with enhanced winter precipitation regimes suggested by Vincent et al. (2005) in this part of the Alps and further support the influence of snowmelt on soil erosion and runoff in the drainage basin of LBH. This peak may also partly result from soils erosion induced by the maximal advance of glaciers during the Holocene (ca 2700 m a.s.l., according to Flusin et al., 1909 and Edouard, 1994). The Medieval Climate Anomaly (MCA) is, on the contrary, characterized by a relatively dry climate and high summer temperatures in European Alps (Büntgen et al., 2011; Corona et al., 2011). Such conditions may have favoured snowmelt erosion and thus soil supply in LBH06, but the highest peak of soil particles during the MCA is also contemporaneous with a short period around AD1050 characterized by wetter conditions in front of the Alps (Leroux et al., 2008; Magny et al., 2011). Such wetter conditions may have therefore further enhanced runoff in the drainage basin of LBH during the MCA.

In summary, soil supply in LBH06 during the Holocene is resulting from runoff and seems to be a reliable proxy to detect wet periods at high altitude in the Grandes Rousses Massif. More humid periods during the Late Holocene and higher soil organic fraction supply in LBH are also matching higher peak in algal production. Following Reynolds et al. (2000), soil supply to LBH may have thus also promoted nutrients loadings and favoured algal productivity.
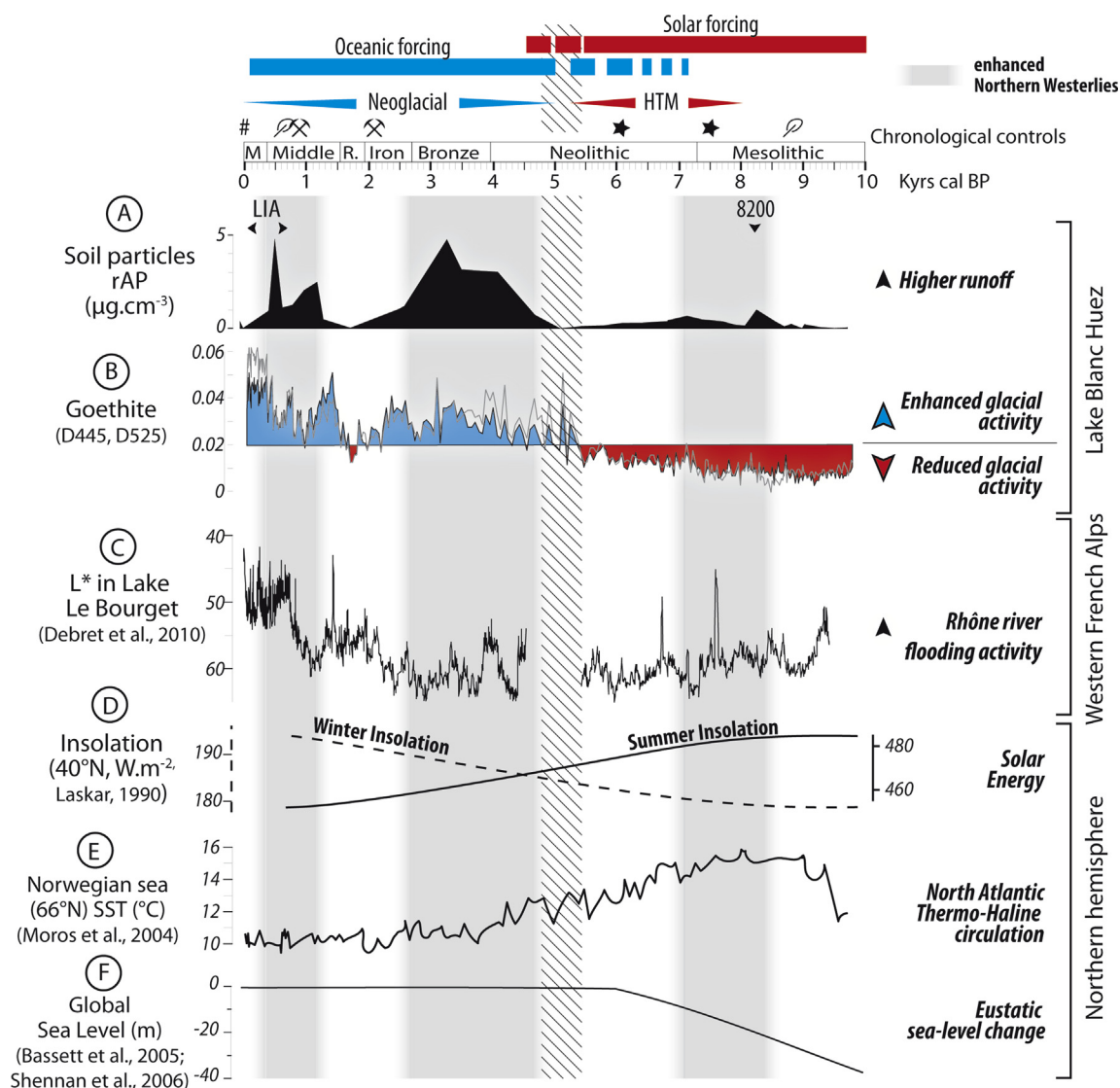
Fig. 8. Global climate forcing during the Holocene (A) from Debret et al. (2009) is compared with soil particles content (rAP) in LBH06 (core without event layers) interpreted as a runoff process marker (B). The goethite occurrence (D445, D525) in LBH06 (core without event layers) (C) can be used as a proxy of glacial activity in its catchment area. The Rhone river flooding activity (D) from Debret et al. (2010), together with the solar energy (E) from Laskar (1990), the North-Atlantic circulation evolution over the Holocene (F), reflected by sea surface temperature (SST) in the North Atlantic from Moros et al. (2004), and the eustatic sea-level change (G) from Bassett et al. (2005) and Shennan et al. (2006) are also compared.

5.4. Evolution of human impact at high-altitude

In short core LBH03, Chapron et al. (2007) have previously identified the impact on the environment of the development of Alpe d'Huez ski resort during the last century. Based on measurements of the Ag/Sr ratio in LBH06 lacustrine sediments, both Garçon et al. (2012) and this study precise the impacts of Middle Age mining activities next to the lake, documented between AD1150 and AD1339 (Bailly-Maître and Bruno-Dupraz, 1994). The end of this period of mining exploitation is synchronous with a phase of enhanced glacial activity in the catchment of LBH dated from AD1300 (Fig. 7D) and corresponding to the onset of the Little Ice Age. This suggests a potential climatic control on recent human activities in high-altitude sites. Our results also suggest that this recent phase of human mining exploitation was not the first as the evolution of the Ag/Sr ratio in LBH06 (Fig. 6C) highlights a previous peak dated from the Iron Age by Bailly-Maître and Bruno-Dupraz

(1994). Since we do not observe any phase of soil erosion during these two periods of mining activities, it seems, however, that such human activities did not disturbed the paedogenetic cover (Fig. 7G). Soil erosion is therefore only attributed to climatic forcing and wetter climate. In contrast, the two periods of mining exploitation are associated with higher content in upper vegetation debris (LCF, Fig. 7G). Since LBH is located above the timberline, this higher content in upper vegetation debris could be attributed to the extraction of the ore using wood fires (Bailly-Maître and Bruno-Dupraz, 1994) and the necessity of combustible material such as wood originating from lower altitudes.

5.5. Climate forcing on Holocene high-altitude alpine environments

This study proposes the first continuous, high-resolution record of Holocene glacier fluctuations in the western French Alps. Results highlight a long-term bimodal trend from the warm and dry Early

Holocene, characterized by reduced glacial activity, which progressively shifts toward the cooler and wetter Neoglacial period, characterized both by a gradual glacier readvance into the catchment of LBH, and a progressive increase of soil erosion. As shown in Fig. 8, this major transition begins around 5400 cal BP and follows the progressive decline of summer insolation at 40°N (Laskar, 1990). This pattern might therefore indicate a solar forcing on climate evolution over the Holocene in this part of the Alps. According to Loutre et al. (2004), Wiles et al. (2004) and Gray et al. (2010), a decrease in summer insolation favours both cloud formation and snow accumulation in the high-altitude environments and would thus favours glacier development in our study area. It is also well documented that this solar forcing influenced as well ocean circulation associated with melt water from retreating ice sheets (Rimbu et al., 2003; Moros et al., 2004; Bassett et al., 2005; Shennan et al., 2006). Such melt water discharges induced a gradual weakening of the Atlantic water circulation, resulting in a progressive decrease of sea surface temperature (SST) in the North Atlantic, and a raise of the global sea level (Fig. 8). Following Rimbu et al. (2003), Anderson et al. (2004) and Wanner et al. (2008), the continuously decreasing trend both in summer insolation and SST in the North Atlantic could result from a reorganization of atmospheric and/or oceanic circulations. It has been previously suggested that such a shift in climate forcing during the mid-Holocene from solar to ocean-atmosphere coupling would lead to a wetter climate through Western Europe, excepted in the Mediterranean Basin, and favour negative NAO phases (Rimbu et al., 2003; Wanner et al., 2008). According to Casty et al. (2005), negative NAO phases are significantly increasing winter precipitations and are thus impacting the alpine winter climate, in particular at high-altitude. The LBH record of Holocene glacier activity in the western Alps (Fig. 8) seems therefore to reflect large scale climate forcing that affected the Northern hemisphere and the North Atlantic Ocean. The progressive return of glacier activity in the catchment of LBH since the onset of the Neoglacial around 4700 cal BP much probably resulted from the combination of a decreasing trend of summer insolation (limiting snowmelt and favouring ice formation) and enhanced moisture supply from the North Atlantic Ocean to the Western Alps through the northern westerly wind belt.

Irregular short-time scale fluctuations of glacial activity (Fig. 8) are also superimposed on this bimodal trend of the LBH record. We particularly highlight three wetter time-intervals, characterized by higher runoff and enhanced glacier activity (since the onset of the Neoglacial). They are dated from 8700 to 7000, 4700 to 2500 and 1300 to 200 cal BP (grey bands, Fig. 8). These periods are reflecting rapid climate changes involving regional summer cooling and more global reorganization of atmospheric and oceanic circulations in the Northern hemisphere (Larsen et al., 2012 and references therein). Following Wanner et al. (2008), Marzeion and Nesje (2012) and Guyard et al. (2013), we suggest that these periods of higher runoff in the catchment of LBH are reflecting changes in the alpine climate and in particular snow accumulation patterns that are typical from negative NAO phases. Results suggest that such wetter patterns culminated during the Little Ice Age (Fig. 8). Enhanced winter precipitation regimes during these periods could therefore reflect enhanced northern Westerlies across the North Atlantic Ocean.

6. Conclusions

Continuous Holocene glacial and high-altitude alpine environments fluctuations in the Western French Alps were obtained from sedimentological, minerogenic and organic signals in proglacial lacustrine sediment infills from LBH.

First occurrence of paedological organic matter at the base of core LBH clearly indicate that paedogenesis at high altitude started before ca 12 400 cal BP in this part of the Alps. The last occurrence of a glacier at the base of the lake basin is attested by a subaquatic moraine retrieved in the lower part of core LBH and dated between 12 400 and 9700 cal BP. This glacier might thus be either contemporaneous to the Younger Dryas or the Preboreal chronozones and might correspond to the Egesen maximum identified in different part of the Alps by several studies.

Both signals show evidence of reduced glacier activity during the warmth Early Holocene from 9700 to 5400 cal BP. This period of reduced glacier activity is defined by the occurrence of a gyttja facies into the lake. It is however interrupted by one wetter time-interval that initiated higher runoff processes and higher soil erosion, between 8700 and 7000 cal BP. The transition to the Neoglacial period is recorded from 5400 to 4700 cal BP at LBH. It is characterized by a gradual increase of glacial activity after ca 5400 cal BP. After ca 4700 cal BP, glaciers remained present in the catchment area of LBH, as shown by the continuous fine grained material and the iron oxide rich supply. Two wetter phases of significant runoff and soil erosion are dated from 4700 to 2500 and 1300 to 200 cal BP. They suggest important climatic pejorations during these two time intervals which drastically contrast with the Iron Age and the Roman period, which are drier periods, during which no soil erosion is observed. Besides, these two periods are correlated with reduced glacial activities, suggesting a climatic control of high-altitude human activities close to LBH.

Periods of higher runoff processes and higher soil erosion recorded in LBH06 during the Holocene are likely due to enhanced northern Westerlies across the North Atlantic Ocean and further suggest that the LBH06 record is sensitive to large scale climate forcing.

References

Alley, R.B., Agustsdottir, A.M., 2005. The 8k event: cause and consequences of a major Holocene abrupt climate change. Quat. Sci. Rev. 24, 1123–1149.

Alley, R.B., Mayewski, P.A., Sowers, T., Stuiver, M., Taylor, K.C., Clark, P.U., 1997. Holocene climatic instability: a prominent, widespread event 8200 yr ago. Geology 25, 483–486.

Anderson, C., Koc, N., Moros, M., 2004. A highly unstable Holocene climate in the subpolar North Atlantic: evidence from diatoms. Quat. Sci. Rev. 23, 2155–2166.

Anselmetti, F.S., Bühler, R., Finger, D., Girardclos, S., Lancini, A., Rellstab, C., Sturm, M., 2007. Effects of Alpine hydropower dams on particle transport and lacustrine sedimentation. Aquat. Sci. 69, 179–198.

Ariztegui, D., Farrimond, P., McKenzie, J.A., 1996. Compositional variations in sedimentary lacustrine organic matter and their implications for high alpine Holocene environmental changes: Lake St Moritz, Switzerland. Org. Geochem. 24, 453–461.

Ariztegui, D., Bianchi, M.M., Masaferro, J., Lafargue, E., Niessen, F., 1997. Inter-hemispheric synchrony of late-glacial climatic instability as recorded in proglacial Lake Mascardi, Argentina. J. Quat. Sci. 12 (4), 333–338.

Arnaud, F., Révillon, S., Debret, M., Revel, M., Chapron, E., Jacob, J., Giguet-Covex, C., Poulenard, J., Magny, M., 2012. Lake Bourget regional erosion patterns reconstruction reveals Holocene NW European Alps soil evolution and paleohydrology. Quat. Sci. Rev. 51, 81—92.

Bailly-Maître, M.C., Bruno-Dupraz, J., 1994. Brandes en Oisans: la mine d'argent des Dauphins (XII-XIV e s) Isère. Doc. d'Archéol. Rhône-Alpes 9, 172.

Bailly-Maître, M.C., Gonon, T., 2006. L'exploitation de chalcopyrite à l'Âge du Bronze dans le massif des Rousses (Oisans, Isère). In: Proceeding of the 131st Congress of the CTHS. "Tradition et innovation". Grenoble.

Barfety, J.C., Bordet, P., Carme, F., Debelmas, J., Meloux, M., Mont-Juvent, G., 1972a. Carte géologique de Vizille au 1/50000 n° 797. BRGM Edition.

Barfety, J.C., Bordet, P., Carme, F., Debelmas, J., Meloux, M., Mont-Juvent, G., 1972b. Carte géologique de Vizille au 1/50 000—n°797.

Bassett, S.E., Milne, G.A., Mitrovica, J.X., Clark, P.U., 2005. Ice sheet and solid earth influences on far-field sea-level histories. Science 309, 925—928.

Blanchet, G., 1994. Chronique climatologique : Le temps dans la région Rhône-Alpes en 1990. Rev. géogr. Lyon 69, 89—103.

Blaauw, M., 2010. Methods and code for classical age-modelling of radiocarbon sequences. Quat. Geochronol. 5, 512—518.

Büntgen, U., Tegel, W., Nicolussi, K., McCormick, M., Frank, D., Trouet, V., Kaplan, J.O., Herzig, F., Heussner, K.U., Wanner, H., Luterbacher, J., Esper, J., 2011. 2500 years of European climate variability and human susceptibility. Science 331, 578—582.

Burga, C.A., Krusi, B., Egli, M., Wernli, M., Elsener, S., Ziefle, M., Fischer, T., Mavris, C., 2010. Plant succession and soil development on the foreland of the Morteratsch glacier (Pontresina, Switzerland): straight forward or chaotic? Flora 205, 561—576.

Carnelli, A.L., Theurillat, J.P., Thinon, M., Vadi, G., Talon, B., 2004. Past uppermost tree limit in the Central European Alps (Switzerland) based on soil and soil charcoal. Holocene 14, 393—405.

Carozza, L., Chapron, E., Simonneau, A., Mille, B., Guyard, H., St-Onge, G., Rostan, P., Bourgarit, D., Burens, A., 2009. Glacial fluctuations and exploitation of copper resources in high mountain during the late Neolithic and Bronze Age in the French Alps (2500—1500 BC). In: Proceedings for the 1st Mining in European History—Conference of the SFB-HIMAT, 12—15. November 2009, Innsburck, Austria, pp. 81—88.

Casty, C., Wanner, H., Luterbacher, J., Esper, J., Böhm, R., 2005. Temperature and precipitation variability in the European Alps since 1500. Int. J. Climatol. 25, 1855—1880.

Chapron, E., van Resbergen, P., Beck, C., de Batist, M., Paillet, A., 1996. Lacustrine sedimentary records of brutal events in Lake Le Bourget (Northwestern Alps-Southern Jura). Quaternaire 7, 155—168.

Chapron, E., Beck, C., Pourchet, M., Deconninck, J.F., 1999. 1822 earthquake-triggered homogenite in Lake Le Bourget (NW Alps). Terra Nova 11, 86—92.

Chapron, E., van Rensbergen, P., de Batist, M., Beck, C., Henriet, J.P., 2004. Fluid-escape features as a precursor of a large sublacustrine sediment slide in Lake Le Bourget, NW Alps, France. Terra Nova 16, 305—311.

Chapron, E., Arnaud, F., Noël, H., Revel, M., Desmet, M., Perdereau, L., 2005. Rhone River flood deposits in Lake Le Bourget: a proxy for Holocene environmental changes in the NW Alps, France. Boreas 34, 404—416.

Chapron, E., Faïn, X., Magnad, O., Charlet, L., Debret, M., Mélières, M.A., 2007. Reconstructing recent environmental changes from proglacial lake sediments in the Western Alps (Lake Blanc Huez, 2543 m a.s.l. Grandes Rousses Massif, France). Palaeogeogr. Palaeoclimatol. Palaeoecol. 252, 586—600.

Chapron, E., Bailly-Maître, M.C., Anselmetti, F.S., Guyard, H., Saint-Onge, G., Desmet, M., Chauvel, C., Winiarski, T., Magnad, O., Arnaud, F., Charlet, L., Deline, P., Magny, M., Mélières, M.A., 2008. Impact des fluctuations glaciaires et des anciennes activités minières d'altitude sur la sédimentation lacustre proglaciaire au cours du Tardiglaciaire et de l'Holocène dans le massif des Grandes Rousses — Alpes occidentales, France. Cah. Paléoenviron. Collect. Edytem 6, 39—50.

Chapron, E., Dietrich, M., Beck, C., Van Rensbergen, P., Finck, H.P., Menard, G., Nicoud, G., Lemeille, F., Anselmetti, F., De Batist, M., 2009. High-amplitude reflections in proglacial lacustrine basin fills of the NW Alps: origin and implications. In: Bard, P.Y., Chaljub, E., Cornou, C., Cotton, F., Gueguen, P. (Eds.), Proceedings of the Third International Symposium on the Effects of Surface Geology on Seismic Motion, ESG Grenoble, Aout 2006, vol. 2, pp. 1587—1596.

Chardon, M., 1991. L'évolution tardiglaciaire et holocène des glaciers et de la végétation autour de l'Alpe d'Huez (Oisans, Alpes Françaises). Rev. géogr. alpine 79, 39—53.

Combaz, A., 1964. Les palynofaciès. Rev. Micropaléontol. 7, 205—218.

Copard, Y., Di Giovanni, C., Martaud, T., Albéric, P., Olivier, J.E., 2006. Using Rock-Eval 6 pyrolysis for tracking fossil organic carbon in modern environments: implications for the roles of erosion and weathering. Earth Surf. Process. Landf. 31, 135—153.

Corona, C., Edouard, J.L., Guibal, F., Guiot, J., Bernard, S., Thomas, A., Denelle, N., 2011. Long-term summer (AD751—2008) temperature fluctuation in the French Alps based on tree-ring data. Boreas 40, 351—366.

Dahl, S.O., Bakke, J., Lie, Ø., Nesje, A., 2003. Reconstruction of former glacier equilibrium-line altitudes based on proglacial sites: an evaluation of approaches and selection of sites. Quat. Sci. Rev. 22, 275—287.

Dearing, J.A., Jones, R.T., 2003. Coupling temporal and spatial dimensions of global sediment flux through lake and marine sediment records. Glob. Planet. Change 39, 147—168.

Deaton, B.C., Balsam, W.L., 1991. Visible spectroscopy — a rapid method for determining hematite and goethite concentration in geological materials. J. Sediment. Petrol. 61, 628—632.

Debret, M., Desmet, M., Balsam, W., Copard, Y., Francus, P., Laj, C., 2006. Spectrophotometer analysis of Holocene sediments from an anoxic fjord: Saanich Inlet, British Columbia, Canada. Mar. Geol. 229, 15—28.

Debret, M., Sebag, D., Crosta, X., Massei, N., Petit, J.R., Chapron, E., Bout-Roumazeilles, V., 2009. Evidence from wavelet analysis for a mid-Holocene transition in global climate forcing. Quat. Sci. Rev. 28, 2675—2688.

Debret, M., Chapron, E., Desmet, M., Rolland-Revel, M., Magand, O., Trentesaux, A., Bout-Roumazeille, V., Nomade, J., Arnaud, F., 2010. North western Alps Holocene paleohydrology recorded by flooding activity in Lake Le Bourget, France. Quat. Sci. Rev. 29, 2185—2200.

Deline, P., Orombelli, G., 2005. Glacier fluctuations in the western Alps during the Neoglacial, as indicated by the Miage morainic amphitheatre (Mont Blanc massif, Italy). Boreas 34, 456—467.

Desmet, M., Mélières, M.A., Arnaud, F., Chapron, E., Lotter, A.F., 2005. Holocene climates in the Alps: towards a common framework — an introduction. Boreas 34, 401—403.

Di Giovanni, C., Disnar, J.R., Campy, M., Bichet, V., Guillet, B., 1998. Geochemical characterization of soil organic matter and variability of a post glacial detrital organic supply (Chaillexon lake, France). Earth Surf. Process. Landf. 23, 1057—1069.

Di Giovanni, C., Disnar, J.R., Bichet, V., Campy, M., 2000. Seasonal variability and threshold effects of the organic detrital sedimentation in lakes: imbalances between organic records and climatic fluctuations (Chaillexon basin, Doubs, France). Bull. Soc. géol. Fr. 171, 533—544.

Edouard, J.L., 1994. Les lacs d'altitude dans les Alpes françaises. Contribution à la connaissance des lacs d'altitude et à l'histoire des milieux montagnards depuis la fin du Tardiglaciaire. HDR, Université de Grenoble, p. 790.

Fanetti, D., Anselmetti, F.S., Chapron, E., Sturm, M., Vezzoli, L., 2008. Megaturbidite deposits in the Holocene basin fill of Lake Como (Southern Alps, Italy). Palaeogeogr. Palaeoclimatol. Palaeoecol. 259, 323—340.

Fiore, J., Girardclos, S., Pugin, A., Gorin, G., Wildi, W., 2011. Würmian deglaciation of western Lake Geneva (Switzerland) based on seismic stratigraphy. Quat. Sci. Rev. 30 (3—4), 377—393.

Flusin, G., Jacob, C., Offner, J., 1909. Etudes glaciaires, géographiques et botaniques dans le massif des Grandes Rousses, p. 112.

Garçon, M., Chauvel, C., Chapron, E., Fain, X., Lin, M.F., Campillo, S., Bureau, S., Desmet, M., Bailly-Maître, M.C., Charlet, L., 2012. Silver and lead in high-altitude lake sediments: proxies for climate changes and human activities. Appl. Geochem. 27, 760—773.

Gratuze, B., Blet-Lemarquand, M., Barrandon, J.N., 2001. Mass spectrometry with laser sampling: a new tool to characterize archaeological materials. J. Radioanal. Nucl. Chem. 247, 645—656.

Gray, L.J., Beer, J., Geller, M., Haigh, J.D., Lockwood, M., Matthes, K., Cubasch, U., Fleitmann, D., Harrison, G., Hood, L., Luterbacher, J., Meehl, G.A., Shindell, D., van Geel, B., White, W., 2010. Solar influences on climate. Rev. Geophys. 48, 1—43.

Graz, Y., 2009. Production et devenir du carbone organique fossile libéré par les altérations mécaniques et chimiques des formations marneuses : exemple des « terres noires » des bassins versants expérimentaux de Draix (Alpes de Haute Provence, France). Université d'Orléans.

Graz, Y., Di Giovanni, C., Copard, Y., Laggoun-Défarge, F., Boussafir, M., Lallier-Vergès, E., Baillif, P., Perdereau, L., Simonneau, A., 2010. Quantitative palynofacies analysis as a new tool to study transfers of fossil organic matter in recent terrestrial environments. Int. J. Coal Geol. 84, 49—62.

Graz, Y., Di Giovanni, C., Copard, Y., Elie, M., Faure, P., Laggoun-Defarge, F., Lévèque, J., Michels, R., Olivier, J.E., 2011. Occurrence of fossil organic matter in modern environments: optical, geochemical and isotopic evidence. Appl. Geochem. 26, 1302—1314.

Guyard, H., Chapron, E., St-Onge, G., Anselmetti, F.S., Arnaud, F., Magand, O., 2007. High-altitude varves records of abrupt environmental changes and mining activity over the last 4000 years in the Western French Alps (Lake Bramant, Grandes Rousses massif). Quat. Sci. Rev. 26, 2644—2660.

Guyard, H., Chapron, E., St-Onge, G., Francus, P., Labrie, J., 2013. Late Holocene NAO and oceanic forcing on high-altitude alpine proglacial sedimentation (Lake Bramant, Western French Alps). Holocene 23 (8), 1163—1172.

Haas, J.N., Richoz, I., Tinner, W., Wick, L., 1998. Synchronous Holocene climatic oscillations recorded on the Swiss Plateau and at timberline in the Alps. Holocene 8, 301—309.

Hansen, K., 1959. The terms Gyttja and Dy. Hydrobiologia 13, 309—315.

Holzhauser, H., Zumbühl, H.J., 1999. Glacier fluctuations in the western Swiss and Franch Alps in the 16th century. Clim. Change 43, 223—237.

Holzhauser, H., Magny, M., Zumbühl, H.J., 2005. Glacier and lake-level variations in west-central Europe over the last 3500 years. Holocene 15, 789—801.

Hormes, A., Müller, B.U., Schlüchter, C., 2001. The Alps with little ice: evidence for eight Holocene phases of reduced glacier extent in the Central Swiss Alps. Holocene 11, 255—265.

IUSS, Working Group WRB, 2006. World Reference Base for Soil Resources 2006.

Ivy-Ochs, S., Kerschner, H., Maisch, M., Christi, M., Kubik, P.W., Schluchter, C., 2009. Latest Pleistocene and Holocene glacier variations in the European Alps. Quat. Sci. Rev. 28, 2137—2149.

Joerin, U.E., Stocker, T.F., Schlüchter, C., 2006. Multicentury glacier fluctuations in the Swiss Alps during the Holocene. Holocene 16, 697—704.

Jungclaus, J.H., Lorenz, S.J., Timmreck, C., Reick, C.H., Brovkin, V., Six, K., Segschneider, J., Giorgetta, M.A., Crowley, T.J., Pongratz, J., Krivova, N.A., Vieira, L.E., Solanki, S.K., Klocke, D., Botzet, M., Esch, M., Gayler, V., Haak, H., Raddatz, T.J., Roeckner, E., Schnur, R., Widmann, H., Claussen, M., Stevens, B.,

Marotzke, J., 2010. Climate and carbon-cycle variability over the last millennium. Clim. Past 6, 723—737.

Lajeunesse, P., St-Onge, G., 2008. The subglacial origin of the lake Agassiz-Ojibway final outburst flood. Nat. Geosci. 1, 184—188.

Lallier-Vergès, E., Sifeddine, A., de Beaulieu, J.L., Reille, M., Tribovillard, N., Bertrand, P., 1993. Sensibilité de la sédimentation organique aux variations climatiques du Tardi-Würm et de l'Holocène ; le lac du Bouchet (Haute-Loire, France). Bull. Soc. Géol. Fr. 164, 661—673.

Larsen, D.J., Miller, G.H., Geisdóttir, Á., Ólafsdóttir, S., 2012. Non-linear Holocene climate evolution in the North Atlantic: a high-resolution, multi-proxy record of glacier activity and environmental change from Hvítárvatn, central Iceland. Quat. Sci. Rev. 39, 14—25.

Laskar, J., 1990. The chaotic motion of the solar system: a numerical estimate of the size of the chaotic zones. Icarus 88, 266—291.

Lauterbach, S., Chapron, E., Brauer, A., Hüls, M., Gilli, A., Arnaud, F., Piccin, A., Nomade, J., Desmet, M., von Grafenstein, U., 2012. A sedimentary record of Holocene surface runoff events and earthquake activity from Lake Iseo (Southern Alps, Italy). Holocene 22, 749—760.

Leeman, A., Niessen, F., 1994. Holocene glacial activity and climatic variations in the Swiss Alps: reconstructing a continuous record from proglacial lake sediments. Holocene 4, 259—268.

Leroux, A., Bichet, V., Walter-Simonnet, A.V., Magny, M., Adatte, T., Gauthier, E., Richard, H., Baltzer, A., 2008. Late-Glacial Holocene sequence of Lake Saint-Point (Jura Mountains, France): detrital inputs as records of climate change and anthropic impact. C. R. Geosci. 340, 883—892.

Leonard, E.M., 1997. The relationship between glacial activity and sediment production: evidence from a 4450-year varve record of neoglacial sedimentation in Hector Lake, Alberta, Canada. J. Paleolimnol. 17, 319—330.

Libby, W.F., 1967. History of Radiocarbon Dating. University of Chicago Press, p. 22.

Loutre, M.F., Paillard, D., Vimeux, F., Cortijo, E., 2004. Does mean annual insolation have the potential to change the climate? Earth Planet. Sci. Lett. 221, 1—14.

Magny, M., 2004. Holocene climate variability as reflected by mid-European lake-level fluctuations and its probable impact on prehistoric human settlements. Quat. Int. 113, 65—79.

Magny, M., Peyron, O., Gauthier, E., Vannière, B., Millet, L., Vermot-Desroches, B., 2011. Quantitative estimates of temperature and precipitation changes over the last millenium from pollen and lake-level data at Lake Joux, Swiss Jura Mountains. Quat. Res. 75, 45—54.

Marzeion, B., Nesje, A., 2012. Spatial patterns of North Atlantic Oscillation influence on mass balance variability of European glaciers. Cryosphere 6, 661—673.

Matthews, J.A., Karlén, W., 1992. Asynchronous neoglaciation and Holocene climatic change reconstructed from Norwegian glaciolacustrine sedimentary sequences. Geology 20, 991—994.

Meteo France, 2008. http://www.alertes-meteo.com/cartes/precipitations-annuelles.php.

Meyers, P.A., Ishiwatari, R., 1993. Lacustrine organic geochemistry — an overview of indicators of organic-matter sources and diagenesis in lake sediments. Org. Geochem. 20, 867—900.

Montjuvent, G., Chardon, M., 1989. Les extensions glaciaires des versants ouest et sud des Grandes Rousses. CNRS/Université de Grenoble.

Moros, M., Emeis, K., Risebrobakken, B., Snowball, I., Kuijpers, A., McManus, J., Jansen, E., 2004. Sea surface temperatures and ice rafting in the Holocene North Atlantic: climate influences on northern Europe and Greenland. Quat. Sci. Rev. 23, 2113—2126.

Moscariello, A., Pugin, A., Wildi, W., Beck, C., Chapron, E., de Batist, M., Girarclos, S., Ivy Ocks, S., Rachoud-Schneider, A.M., Signer, C., van Clauwenberghe, T., 1998. Déglaciation würmienne dans des conditions lacustres à la terminaison occidentale du bassin lémanique (Suisse occidentale et France). Eclogae Geol. Helv. 91, 185—201.

Mulder, T., Cochonat, P., 1996. Classification of offshore mass movements. J. Sediment. Res. 66, 43—57.

Mulder, T., Chapron, E., 2011. Flood deposits in continental and marine environments: character and significance. In: Slatt, R.M., Zavala, C. (Eds.), Sediment Transfer from Shelf to Deep Water. Revisiting the Delivery System, AAPG Studies in Geology, 61, pp. 1—30.

Nesje, A., Matthews, J.A., Dahl, S.O., Berrisford, M.S., Andersson, C., 2001. Holocene glacier fluctuations of Flatebreen and winter-precipitation changes in the Jostedalsbreen region, western Norvay, based on glaciolacustrine sediment records. Holocene 11, 267—280.

Noël, H., Garbolino, E., Brauer, A., Lallier-Vergès, E., de Beaulieu, J.L., Disnar, J.R., 2001. Human impact and soil erosion during the last 5000 yrs as recored in lacustrine sedimentary organic matte rat Lac d'Annecy, the French Alps. J. Paleolimnol. 25, 229—244.

Nomade, J., Chapron, E., Desmet, M., Reyss, J.L., Arnaud, F., Lignier, V., 2005. Reconstructing historical seismicity from lake sediments (Lake Laffrey, Western Alps, France). Terra Nova 117, 350—357.

Ollesch, G., Kistner, I., Meissner, R., Lindenschmidt, K.E., 2006. Modelling of snowmelt erosion and sediment yield in a small low-mountain catchment in Germany. Catena 68, 131—176.

Patience, A.J., Lallier-Vergès, E., Sifeddine, A., Albéric, P., Guillet, B., 1995. Organic fluxes and early diagenesis in the lacustrine environment. In: Lallier-Vergès, E., Tribovillard, N., Bertrand, P. (Eds.), Organic Matter Accumulation, Lecture Notes in Earth Sciences, vol. 57. Springer, Heidelberg, pp. 145—156.

Poulenard, J., Podwojewski, P., 2003. Alpine soils. In: Dekker, M. (Ed.), Encyclopedia of Soil Science.

Reimer, P.J., Baillie, M.G.L., Bard, E., Bayliss, A., Beck, J.W., Blackwell, P.G., Bronk Ramsey, C., Buck, C.E., Burr, G.S., Edwards, R.L., Friedrich, M., Grootes, P.M., Guilderson, T.P., Hajdas, I., Heaton, T.J., Hogg, A.G., Hughen, K.A., Kaiser, K.F., Kromer, B., McCormac, F.G., Manning, S.W., Reimer, R.W., Richards, D.A., Southon, J.R., Talamo, S., Turney, C.S.M., van der Plicht, J., Weyhenmeyer, C.E., 2009. IntCal09 and Marine09 radiocarbon age calibration curves, 0-50,000 years cal BP. Radiocarbon 51, 1111—1150.

Reynolds, C., Dokulil, M., Padisák, J., 2000. Understanding the assembly of phytoplankton in relation to the trophic spectrum: where are we now? Hydrobiologia 424, 147—152.

Rimbu, N., Lohmann, G., Lorenz, S.J., Kim, J.H., Schneider, R.R., 2003. Holocene climate variability as derived from alkenone sea surface temperature and coupled ocean-atmosphere model experiments. Clim. Dyn. 23, 215—227.

Schnellmann, M., Anselmetti, F.S., Giardini, D., McKenzie, J.A., 2006. 15,000 Years of mass-movement history in Lake Lucerne: implications for seismic and tsunami hazards. Eclogae Geol. Helv. 99, 409—428.

Sebag, D., Disnar, J.R., Guillet, B., Di Giovanni, C., Verrecchia, E.P., Durand, A., 2005. Monitoring organic matter dynamics in soil profiles by 'Rock-Eval pyrolysis': bulk characterization and quantification of degradation. Eur. J. Soil. Sci. 57, 344—355.

Sebag, D., Copard, Y., Di Giovanni, C., Durand, A., Laignel, B., Ogier, S., Lallier-Verges, E., 2006. Palynofacies as useful tool to study origins and transfers of particulate organic matter in recent terrestrial environments: synopsis and prospects. Earth-Sci. Rev. 79, 241—259.

Seierstad, J., Nesje, A., Dahl, S.O., Simonsen, J.R., 2002. Holocene glacier fluctuations of Grovabreen and Holocene snow-avalanche activity reconstructed from lake sediments in Grningstlsvatnet, western Norway. Holocene 12, 211—222.

Shennan, I., Bradley, S., Milne, G., Brooks, A., Bassett, S., Hamilton, S., 2006. Relative sea-level changes, glacial isostatic modelling and ice-sheet reconstructions from the British Isles since the Last Glacial Maximum. J. Quat. Sci. 21, 585—599.

Sifeddine, A., Bertrand, P., Lallier-Vergès, E., Patience, A.J., 1996. Lacustrine organic fluxes and palaeoclimatic variations during the last 15 ka: Lac du Bouchet (Massif Central, France). Quat. Sci. Rev. 15, 203—211.

Simonneau, A., Doyen, E., Chapron, E., Millet, L., Vannière, B., Di Giovanni, C., Bossard, N., Tachikawa, K., Bard, E., Albéric, P., Desmet, M., Roux, G., Lajeunesse, P., Berger, J.F., Arnaud, F., 2013a. Holocene land-use evolution and associated soil erosion in the French Prealps inferred from Lake Paladru sediments and archaeological evidences. J. Archaeol. Sci. 40, 1636—1645.

Simonneau, A., Chapron, E., Vannière, B., Wirth, S.B., Gilli, A., Di Giovanni, C., Anselmetti, F.S., Desmet, M., Magny, M., 2013b. Mass-movement and flood-induced deposits in Lake Ledro, Southern Alps, Italy: implications for Holocene palaeohydrology and natural hazards. Clim. Past 9, 825—840.

Simonneau, A., Chapron, E., Courp, T., Tachikawa, K., Le Roux, G., Baron, S., Galop, D., Garcia, M., Di Giovanni, C., Matelica-Heino, M., Mazier, F., Foucher, A., Houet, T., Desmet, M., Bard, E., 2013c. Recent climatic and anthropogenic imprints on lacustrine systems in Pyrenean Mountains inferred from minerogenic and organic clastic supply (Vicdessos valley, Pyrenees, France). Holocene 23 (12), 1764—1777.

Six, D., Reynaud, L., Letréguilly, A., 2007. Bilans de masse des glaciers alpins et scandinaves, leurs relations avec l'oscillation du climat de l'Atlantique nord. Earth Planet. Sci. 333, 693—698.

Talbot, M.R., Livingstone, D.A., 1989. Hydrogen index and carbon isotopes of lacustrine organic matter as lake level indicators. Palaeogeogr. Palaeoclimatol. Palaeoecol. 70, 121—137.

Talon, B., 2010. Reconstruction of Holocene high-altitude vegetation cover in the French Southern Alps: evidence from soil charcoal. Holocene 20, 35—44.

Tanasienko, A.A., Yakutina, O.P., Chumbaev, A.S., 2009. Snowmelt runoff parameters and geochemical migration of elements in the dissected forest-steppe of West Siberia. Catena 78, 122—128.

Tanasienko, A.A., Yakutina, O.P., Chumbaev, A.S., 2011. Effect of snow amount on runoff, soil loss and suspended sediment during periods of snowmelt in southern West Siberia. Catena 87, 45—51.

Thouvenot, F., Fréchet, J., Jenatton, L., Gamond, J.F., 2003. The Belledonne Border fault: identification of an active seismic strike-slip fault in the western Alps. Geophys. J. Int. 155, 174—192.

Torinesi, O., Letréguilly, A., Valla, F., 2002. A century reconstruction of the mass balance of Glacier de Sarennes, French Alps. J. Glaciol. 48, 142—148.

van Rensbergen, P., de Batist, M., Beck, C., Chapron, E., 1999. High-resolution seismic stratigraphy of glacial to interglacial fill of a deep glacigenic lake: Lake Le Bourget, Northwestern Alps, France. Sediment. Geol. 128, 99—129.

Vincent, C., 2002. Influence of climate change over the 20th century on four French glacier mass balances. J. Geophys. Res. 107 (D19), 4375. http://dx.doi.org/10.1029/2001JD000832.

Vincent, C., Le Meur, E., Six, D., 2005. Solving the paradox of the end of the Little Ice Age in the Alps. Geophys. Res. Lett. 32, L09706.

Vollweiler, N., Scholz, D., Mühlinghaus, C., Mangini, A., Spötl, C., 2006. A precisely dated climate record for the last 9 kyr from three high alpine stalagmites, Spannagel Cave, Austria. Geophys. Res. Lett. 33, L20703.

von Grafenstein, U., Erlenkeuser, H., Brauer, A., Jouzel, J., Johnsen, S.J., 1999. A mid-European decadal isotope-climate record from 15,500 to 5000 years B.P. Science 284, 1654—1657.

Wanner, H., Beer, J., Bütikofer, J., Crowley, T.J., Cubasch, U., Flückiger, J., Goose, H., Grosjean, M., Joos, F., Kaplan, J.O., Küttel, M., Müller, S.A., Prentice, I.C., Solomina, O., Stocker, T.F., Tarasov, P., Wagner, M., Widmann, M., 2008. Mid- to Late Holocene climate change: an overview. Quat. Sci. Rev. 27, 1791—1828.

Wentworth, C.K., 1922. A scale of grade and class terms for clastic sediments. J. Geol. 30, 377—392.

Wiles, G.C., D'Arrigo, R.D., Villalba, R., Calkin, P.E., Barclay, D.J., 2004. Century-scale solar variability and Alaskan temperature change over the past millennium. Geophys. Res. Lett. 31, L15203.

Wilhelm, B., Arnaud, F., Enters, D., Allignol, F., Legaz, A., Magand, O., Revillon, S., Giguet-Covex, C., Malet, E., 2011. Does global warming favour the occurrence of extreme floods in European Alps? First evidences from a NW Alps proglacial lake sediment record. Clim. Change 113 (3—4), 563—581.